NAL PROPOSAL No.
Scientific Spokesman: Z.G.T. Guiragossián
High Energy Physics Laborator
W. W. Hansen Laboratories of
Physics
Stanford University
Stanford, California 94305
Telephone: (415) 327-7800 Ext. 333

NAL PROPOSAL FOR

STUDY OF PHOTONS AND LEPTONS PRODUCED IN MESON-NUCLEON COLLISIONS IN THE DEEP SCATTERING REGION; SEARCH FOR INTERMEDIATE BOSONS, HEAVY LEPTONS, ANOMALOUS HADRONIC PROCESSES AND STUDY OF MULTI-GAMMA-RAY FINAL STATES

Submitted by

Z. G. T. Guiragossián, R. Hofstadter, R. F. Schilling, and M. R. Yearian
The W. W. Hansen High Energy Physics Laboratory and Department of Physics
Stanford University, Stanford, California 94305

and

E. V. Hungerford III, G. S. Mutchler, and G. C. Phillips
The T. W. Bonner Nuclear Laboratories and Department of Physics
Rice University, Houston, Texas 77001

and

B. W. Mayes
Department of Physics
The University of Houston, Houston, Texas 77001

October 1972*

*Proposals, 164-I and 164-II were originally submitted together on December 1971. This proposal updates 164-I.

CONTENTS

PROPOSAL TO THE NATIONAL ACCELERATOR LABORATORY

for

Study of Photons and Leptons Produced in Meson-Nucleon Collisions in the Deep Scattering Region; Search for Intermediate Bosons, Heavy Leptons, Anomalous Hadronic Processes and Study of Multi-Gamma-Ray Final States

ABSTRACT

We propose to observe gamma rays and leptons carrying high transverse momentum, in pairs or singles, emerging from meson-nucleon collisions at high energies. These meson-nucleon collisions probe the constituent structure of nucleons and reveal anomalous hadronic interaction processes at small distances. We will search for structure in the effective mass continuum of various (wide angle) pair combinations and in the transverse momentum spectra of singles and pairs. An experimental sensitivity corresponding to a cross section times branching ratio of $\sim 10^{-37} - 10^{-38}$ cm^2 is provided for the production of intermediate bosons, Lee-Wick heavy photons and sequential heavy leptons from meson-nucleon collisions. With a 300 GeV/c meson beam the mass range up to $\sim$ 22 GeV will be explored with good resolution. The forward (small angle) production of multi-gamma-ray final states will be studied systematically with a mass resolution of $< 2\%$, to search for massive bosons and to reveal dynamical properties of multi-gamma-ray states.

I. INTRODUCTION

We have reworked our original meson physics experimental proposal, 164-I, to include a method of probing the constituent structure of nucleons in the deep scattering region by detecting photons and leptons emerging from meson-nucleon collisions. Also, we propose to make a first generation search at NAL for intermediate bosons W, Lee-Wick heavy photons B, and sequential heavy leptons L, from π-N scattering processes.

If the nucleon is a composite system with constituents that exhibit point-like coupling to photons, then certain predictable similarities should exist between hadron-hadron collisions and electron-nucleon scattering in the deep inelastic kinematical region. That is, for hadrons in the deep scattering region of large s and t, at short characteristic distances, the same constituent interactions should prevail once the effect of coherent hadronic exchange mechanisms has subsided. In this framework, long range strong forces are provided by mesonic exchanges at small momentum transfers. Short range forces at the core of hadrons are provided by the interaction of constituents at large momentum transfers.

We are facing some deep and fascinating questions. Some of these are: Are there more fundamental constituents that make up hadrons? What are these constituents--partons, quarks or fragments or other things? Do these have form factors or are these really point-like objects when coupled to photons? Could these exhibit point Fermi interactions? Could these ever exist as free states? These are some of the fundamental questions which we hope to approach experimentally.

As an experimental probe we choose a meson beam of the highest possible energy and intensity: 150-300 GeV and 10^8 - 10^9 π/pulse. This choice is made simply because mesons by definition should be composed of parton-antiparton pairs, whereas nucleons should be composed of partons

predominantly. In particular to study hadron-hadron short range forces of constituents, the choice of a meson beam provides an initial meson-nucleon state in which the parton-antiparton ingredient is enhanced with respect to what may be expected in an initial nucleon-nucleon state. Also, on the average, the quantity x, the fractional momentum of constituents, is higher for mesons ($q\bar{q}$) than it is for nucleons (qqq). Therefore, at NAL we expect to find more copious and energetic $q\bar{q}$ generated products in meson-nucleon collisions than in nucleon-nucleon collisions. If we were to find the reverse, there would immediately be an anomaly. From collisions in both initial states, the detection of high transverse momentum gamma-rays and leptons, in pairs or singles, particularly is interesting because these are the likely by-products of any $q\bar{q}$ annihilation mechanism. At least, the relative comparison of high transverse momentum yields, from meson-nucleon and nucleon-nucleon initial states, will provide several valuable clues to construct theories.

We believe that the study of deep inelastic leptons and gamma-rays from pion-nucleon collisions should be made in conjunction with a similar study for proton-nucleon collisions at NAL. The possibility of anomalous effects in hadronic processes, primarily due to leptonic and electromagnetic interaction of constituents, and the unknown behavior at large transverse momenta, are of sufficiently fundamental interests to support the study at the same time of both pion and proton induced collisions. The pion experiment at NAL is unique because at present, the highest energy meson beams can be made available only at NAL.

With a high intensity pion beam, we propose to make wide angle investigations in order to observe the high transverse momentum inclusive spectra of produced $e^{\pm}$, $\mu^{\pm}$ and γ from pion-nucleon collisions. Also, we propose to use a large acceptance spectrometer configuration, designed to record in coincidence the production of large angle e^+e^-, $\mu^+\mu^-$, $e^{\pm}\mu^{\mp}$, $e^{\pm}\gamma$, $\mu^{\pm}\gamma$ and $\gamma\gamma$ pairs. The effective mass of these pairs will be measured with an accuracy of better than 1%. The transverse momentum spectra of pairs and singles will be examined to search for structure above the continuum, indicating the production of intermediate bosons, heavy leptons, or Lee-Wick heavy photons.

We have designed a high quality 300 GeV electron/pion beam in which the acceptance is 9.5 μster. % $\Delta p/p$ (FW) and the momentum bite is $\pm$ 2%. We calculate the negative pion intensity of this beam and find that in the range of 100 - 300 GeV, 10^8 - 10^9 π^-/pulse are obtained for $\underline{10^{12}}$ interacting protons of 400-500 GeV. With high energy and high intensity, the main other advantage of this beam is that at the fourth focus a spot size of $\pm$ 2mm is obtained, without any loss of beam intensity. At the experimental target, this small spot size allows the use of an efficient and economical spectrometer configuration, with large acceptance and excellent resolution. Therefore, under these conditions the pion-nucleon experiment will have event rates which are competitive with those from other proton-nucleon experiments at NAL. A π^- beam intensity of 10^8 - 10^9 π/pulse and our detector geometrical acceptance of 10 - 20% will provide the equivalent event rate and cover about the same kinematical region as in the proposal of E-70. That particular proton experiment is expected to have a geometrical acceptance of 0.3%, using the external proton beam at 10^{10} - 10^{11} p/pulse.

There are reasons to believe that our experiment can withstand a possible lowering of pion beam intensities. It is expected that in the deep scattering region, the added enhancement of $q\bar{q}$ constituents of the pion-nucleon system would produce higher yields. For example, theoretical estimates predict that deep scattering semileptonic processes in pion-nucleon collisions are two orders of magnitude more probable than in equivalent proton-nucleon collisions. Similarly, deep scattering electromagnetic processes in π-N collisions are about one order of magnitude more probable than in p-N collisions. These considerations are based on the amount of overlapping energetic parton-antiparton pairs which are found in the π-N vs. the p-N initial states. On the other hand, finding the opposite of these expectations immediately would have a dramatic impact on current thinking. Thus, the relative comparison of results from this π-N experiment and other p-N experiments should provide informative sources of new knowledge.

We also propose to study the forward production of multi-gamma-ray final states from high energy pion-nucleon collisions. In a separate configuration using an accurate, large acceptance and highly efficient multi-gamma-ray spectrometer, we propose to search for the existence of massive bosons with a mass resolution of $< 2\%$. A systematic search of new particles will be made up to mass values of about 5 GeV.

While the scope of this experiment has been enlarged, we believe we have done this efficiently and economically, using basically the same set of detectors planned for this experiment and our electron scattering experiment. The major changes are the following:

a) The spectrometer analyzing magnet is redesigned to have superconducting coils at 20 kgauss. The magnet is 15 feet long and the useful aperture is 3 feet wide with a 1 foot gap. The cost of this magnet is estimated to be $150 K. We have the technical capability, manpower and equipment, to build this magnet at HEPL for NAL. This magnet initially used in our pion and electron experiments, would be available at NAL for other purposes.

b) Several multi-wire proportional chamber planes are added in spectrometer configurations, in some cases to provide redundant information on track orbits of large angle scattered electrons or muons.

c) A second spectrometer module, composed of large NaI(Tl)/MWPC combination, is incorporated in a configuration especially optimized to make coincidence measurement of large angle leptonic pairs and also large angle gamma-ray pairs.

d) Muon identifiers are added to the large NaI(Tl)/MWPC spectrometer modules, to include the efficient detection of muons together with electrons and gamma-rays.

We wish to emphasize that our NAL pion and electron experiments are intimately connected not only in the commonality of beams, spectrometers and other experimental facilities but also, most importantly, in the physics. The scaling behavior of nucleon structure functions, so far established only from electron deep scattering experiments, is assumed to prevail in hadron-hadron deep scattering processes, both for electromagnetic or leptonic final states. At NAL we propose to test and establish

the scaling properties in pion-nucleon deep scattering processes from our pion experiment and we also propose to observe and discover any new scaling behavior in electron-nucleon deep scattering processes in our electron experiment. In both cases these experiments will be made at kinematical regions which are unexplored up to the present time. Experimentally, it is by such an efficient comparison that we expect to acquire new knowledge covering the main features of the nucleon constituents.

II. EXPERIMENTAL PROGRAM

1. Meson-Nucleon Collisions in the Deep Scattering Region

We propose to use a high energy and high intensity pion beam at NAL in the energy range of 150-300 GeV and with intensities of 10^8 - 10^9 π/pulse, to observe large transverse momentum gamma rays, electrons and muons, emerging from meson-nucleon collisions.

The following inclusive processes will be studied, using a large acceptance and high resolution spectrometer configuration:

$$\pi^- N \rightarrow \gamma + \text{hadrons} \qquad (1)$$

$$\pi^- N \rightarrow e^{\pm} + \text{hadrons} \qquad (2)$$

$$\pi^- N \rightarrow \mu^{\pm} + \text{hadrons} \qquad (3)$$

Because a negative hadron beam at NAL contains also about 2% of K^- and antiproton components, we propose to tag the beam with two threshold and one differential Cerenkov counters. Therefore, K^- and $\bar{p}$ initiated processes in the deep scattering region will be observed:

$$K^- N \rightarrow \left.\begin{matrix} \gamma \\ e^{\pm} \\ \mu^{\pm} \end{matrix}\right\} + \text{hadrons} \qquad (4) \qquad \bar{p} N \rightarrow \left.\begin{matrix} \gamma \\ e^{\pm} \\ \mu^{\pm} \end{matrix}\right\} + \text{hadrons} \qquad (5)$$

The study of these reactions is designed to reveal new knowledge on the constituent nature of nucleons. This experiment will also provide valuable clues concerning the nature of interactions among the constituents of hadronic matter. At NAL the potential meson beam energy and intensity are such that we will be able to observe the onset of three or more interaction regions. We plan to look for structure in the transverse momentum spectra of the above reaction.

The first break should occur when hadronic exchange processes have subsided and the electromagnetic interaction becomes apparent in the deep scattering region. At NAL, it is in this region where the scaling behavior in π-N collisions will be established or a new phenomenon will be found. We remark that scale invariance in deep hadron-hadron collisions is inferred only from studies made in electron-nucleon collisions. This assumption must be tested both with π-N and p-N deep scattering collisions. This is done best by observing the behavior of time-like photons induced in hadron-hadron collisions. Breakdown of scale invariance would cause a complete rethinking in the nucleon constituent models.

The second break should occur when the above electromagnetic interactions among constituents, in turn, have subsided and the semi-weak interaction becomes apparent in the π-N deep scattering region. We argue that these semi-weak processes among hadronic constituents could become apparent more readily in meson-nucleon collisions than in proton-nucleon scattering processes. The first signature of these semi-weak interactions is found in the observation of yields. In this case, the yield of these very large transverse momentum events would grow linearly with S, provided that these interactions have not yet been saturated by a new anomalous effect.

The invariant cross section of the above processes is given[1] by:

$$\frac{E}{p^2}\frac{d^2\sigma}{dpd\Omega} = \frac{1}{\pi s}\frac{d^2\sigma}{dx_1 dx_2} = \frac{4\pi\alpha^2}{(P_\perp)^4}\frac{F(x_1,x_2)}{\pi} \qquad (6)$$

where x_2 is the fractional momentum transfer, $x_2 = Q^2/s$ and x_1 is the fractional energy, $x_1 = E/E_o$.

$$x_1 x_2 = P_\perp^2/s \quad .$$

In this representation, the function $F(x_1, x_2)$ has an especial significance. This function is the probability measure of finding a parton in one of the hadrons, and an antiparton in the other hadron, such that by the process of their annihilation a byproduct is obtained with the kinematical variable amounts of x_1 and x_2.

Equation (6) applies for the case of electromagnetic interactions among constituents. In the case of semi-weak processes between partons the factor $4\pi\alpha^2/P_\perp^4$ is replaced by $(G\sqrt{2})^2$ where G is the "universal" weak constant: $G \simeq 10^{-5}/M_p^2$.

Interaction diagrams, depicting the constituent annihilation process in hadron-hadron deep scattering collisions, are shown in Fig. 1(a) and 1(b). Also shown are the transverse momentum spectra [Fig. 1(c)] of gamma-rays and electrons which are expected from this theoretical model.

At NAL, there are proposed experiments (see for example, E-70) for the study of large transverse momentum production of gamma-rays and electrons from proton-nucleon collisions:

$$pN \rightarrow \gamma + \text{hadrons} \qquad (7)$$

$$pN \rightarrow e^{\pm} + \text{hadrons} \qquad (8)$$

Although the external proton beam intensity is several orders of magnitude higher than the intensity of our proposed pion beam, we show that in our experiment counting rates are about the same for reactions (1) and (2) as for reactions (7) and (8) in E-70. There are two remarkable advantages supporting this expectation. One is experimental, and it has to do with our geometrical acceptance (10-20%) and pion beam intensity (10^8-10^9 $\pi^-/10^{12}$ protons) versus the experimentally usable proton intensity (10^{10}-10^{11}) and

(A)

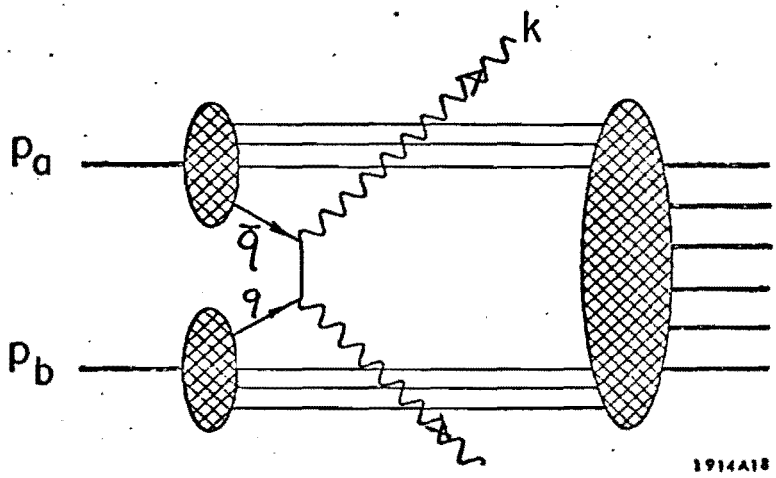
k
p_a
p_b
$\bar{q}$
q
hadrons
1914A18

(B)

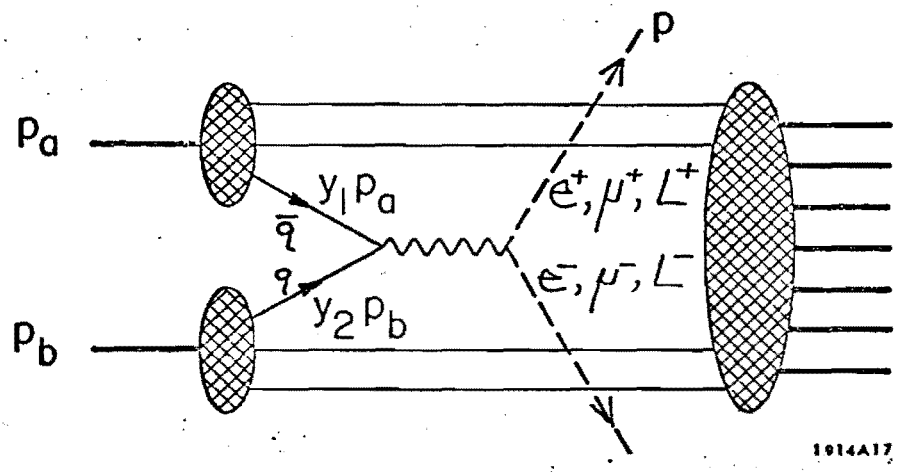
p
p_a
p_b
$y_1 p_a$
$y_2 p_b$
$\bar{q}$
q
e^+, μ^+, L^+
e^-, μ^-, L^-
hadrons
1914A17

(C)

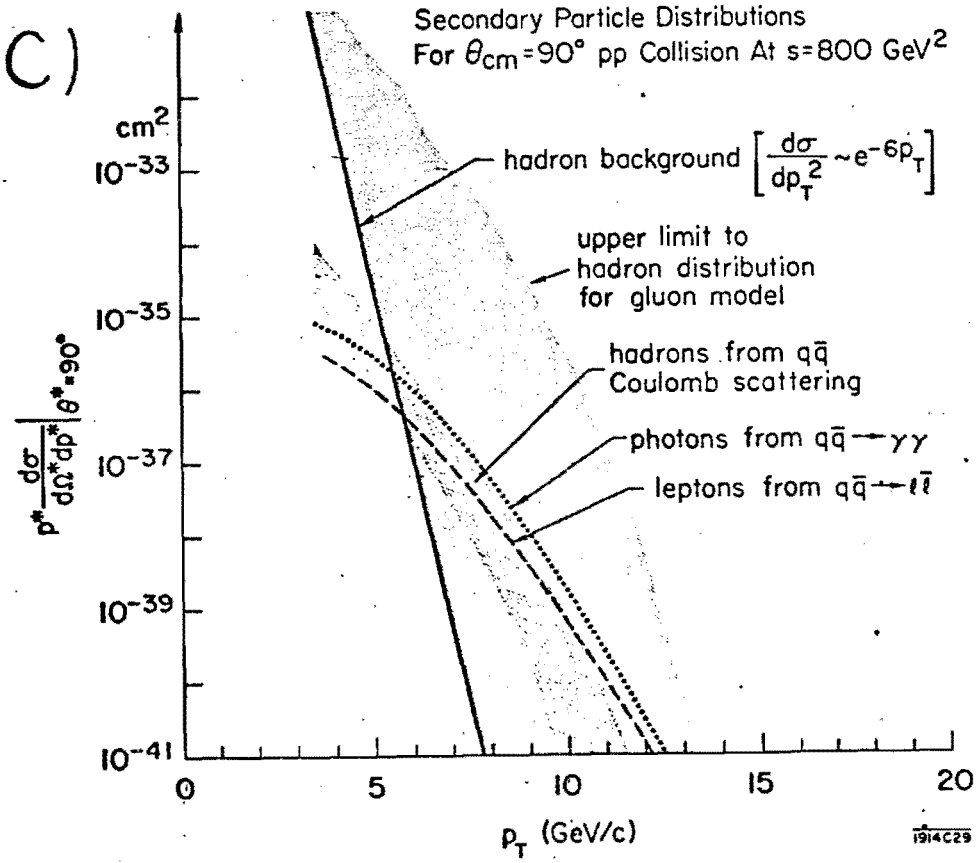
Secondary Particle Distributions
For $\theta_{cm}=90°$ pp Collision At s=800 GeV^2
hadron background $\left[\frac{d\sigma}{dp_T^2} \sim e^{-6p_T}\right]$
upper limit to
hadron distribution
for gluon model
hadrons from $q\bar{q}$
Coulomb scattering
photons from $q\bar{q} \rightarrow \gamma\gamma$
leptons from $q\bar{q} \rightarrow l\bar{l}$
$p^* \frac{d\sigma}{d\Omega^* dp^*}\Big|_{\theta^*=90°}$
cm^2
10^{-33}
10^{-35}
10^{-37}
10^{-39}
10^{-41}
0
5
10
15
20
p_T (GeV/c)
1914C29

Figure 1

the geometrical acceptances in other proton experiments (0.3%). The second is theoretical, which we discuss because of its instructive relevance to both pion and proton experiments. This discussion follows the trend of a recent CERN ISR experiment.

Observation of reaction (7) at the ISR indicate a dramatic behavior. At large and fixed transverse momentum values of the "π^o", the invariant cross section of

$$pp \rightarrow \pi^o \text{ or } \gamma + \text{hadrons} \qquad (9)$$

rises as a function of S. Also, at large $P_\perp$ ("π^o") values, and fixed S, the shape of the invariant cross section behaves according to a known predictable[1] fashion, given by eq. (6) and the calculated[1] form factor of this reaction. This experimental result[2] is shown in Fig. 2. Although the shape of this spectrum is predictable, the experimental cross sections are about a factor of 100 times higher than expected. It is as if α in eq.(6) should have a value of between 0.1 and 1.0, instead of being 1/137. It should be remarked that in the ISR experiment detectors were used where space resolution could not distinguish between the production of single gamma rays and the production of π^o decay gamma-ray pairs at high energies.

Recent theoretical developments which explain the above behavior are based on new notions. There should be a transition between the Feynman scaling region[3] at low $p_\perp$ values and the deep scattering region of interacting constituents[1] at very large $p_\perp$ values. The new types of assumed interactions[4] are 1) the <u>interchange</u> of hadronic constituents coupled by the emission of virtual photons and 2) the hadron's bremsstrahlung which is emission of mesonic radiation. In this framework, the power law fall-off

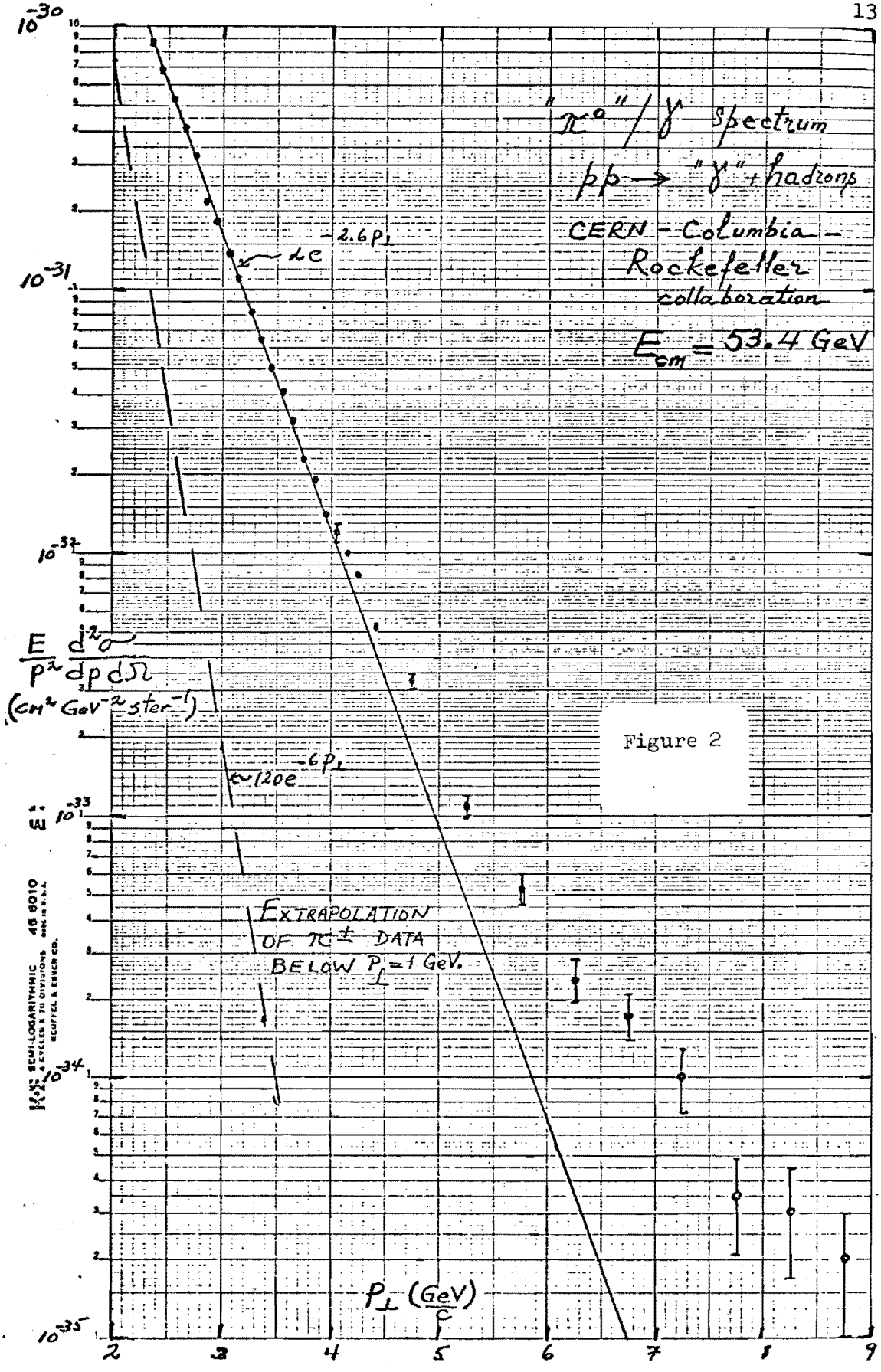
"π⁰" / γ Spectrum
pp → "γ" + hadrons
CERN - Columbia - Rockefeller collaboration
E_cm = 53.4 GeV
~ e^-2.6 p_T
~ e^-6 p_T
EXTRAPOLATION OF π± DATA BELOW P_T = 1 GeV.
E d³σ / p² dp dΩ (cm² GeV⁻² ster⁻¹)
P_T (GeV/c)
55984

Figure 2

in $p_\perp$ is defined by the electromagnetic form factors of interacting hadrons. Thus, the measured nucleon structure functions from e - N deep scattering collisions define the behavior of hadron-hadron interactions. In the deep scattering region the cross sections scale as a function of $P_\perp/\sqrt{s}$ and in the transition zone they behave as:

$$\frac{E}{p^2}\frac{d^2\sigma}{dpd\Omega} = \frac{1}{(P_\perp)^N} F(P_\perp/\sqrt{s}) \qquad (10)$$

A value of N = 8 is predicted[4] for reaction (9) which is found to be in excellent agreement with the ISR results[2]. The same theory predicts a much slower fall-off of yields for our reactions ($N \sim 6$), initiated with pions. The meson-nucleon cross sections at large $p_\perp$ values are much higher than the nucleon-nucleon cross sections due to the differences in the electromagnetic form factors of pions and nucleons.

Therefore, a comparison of pion beam experiments and proton beam experiments at NAL, for large $p_\perp$ and large $P_\perp/\sqrt{s}$ values, is crucial to the fundamental understanding of hadronic interaction mechanisms. For example, if the constituent picture is correct, the π-N yields of reactions (1-3) are much higher; they are not suppressed by the additional form-factor fall-off present in the p-N collisions of reactions (7-8). Finding the opposite of this expectation will be at least very instructive, indicating possibly new anomalous phenomena in hadronic processes for the very large transverse momentum regions.

We emphasize that in this proposed experiment, our multi-gamma-ray spectrometer system will have large acceptance, good space resolution and energy resolution. Hence, at NAL we will have a gamma-ray pair resolution which is restricted only by the natural shower core widths. At high

energies these are typically about 3 cm wide. With great certainty we will be able to distinguish single gamma-rays from π^o decay pairs of gamma-rays, thus resolving the ambiguity in reaction (9).

There is hardly anthing known about the other reactions (2-5) of our proposal, as well as about the proton initiated reaction (8).

We propose to observe pairs of leptons and gamma-rays emerging from π-N deep scattering collisions. The following pair producing reactions will be studied by coincidence measurements with our two-arm spectrometer system:

$$\pi^- N \rightarrow e^+ e^- + \text{hadrons} \qquad (11)$$

$$\pi^- N \rightarrow \mu^+ \mu^- + \text{hadrons} \qquad (12)$$

$$\pi^- N \rightarrow e^{\pm} \mu^{\mp} + \text{hadrons} \qquad (13)$$

$$\pi^- N \rightarrow \gamma_1 \gamma_2 + \text{hadrons} \qquad (14)$$

$$\pi^- N \rightarrow e^{\pm} \gamma + \text{hadrons} \qquad (15)$$

$$\pi^- N \rightarrow \mu^{\pm} \gamma + \text{hadrons} \qquad (16)$$

Only reaction (11) has a counterpart with proposed proton beam experiments:

$$pN \rightarrow e^+ e^- + \text{anything} \qquad (17)$$

We propose to measure the lepton pair cross sections as a function of dilepton mass ($M^2_{\ell\ell'} = Q^2$) and as a function of S in π-N deep scattering collisions. Present knowledge extends only to the dilepton mass region of less than 6 GeV from the study[5] of

$$p + U^{238} \rightarrow \mu^+ \mu^- + \text{anything} \qquad (18)$$

collisions. This study has provided indirect information about dilepton production initiated in p-N collisions and in fact, it cannot be told whether incident protons or secondary pions induced the deep scattering

process in reaction (18). The experiment concerning reaction (18) produced no evidence for structure in the dilepton mass continuum, indicating that the mass of any neutral spin 1 boson which can couple directly like photons, must be greater than 6 GeV. Significant theoretical progress[6] was made however, by explaining the dilepton continuum spectrum of reaction (18) in terms of the nucleon structure functions obtained by

$$e^- N \rightarrow e^- + \text{hadrons} \qquad (19)$$

In the parton-annihilation process of Fig. 1(b), a parton with momentum X_1P_1 from one of the hadrons, annihilates with an antiparton, having momentum X_2P_2 from the other hadron. The deep scattering process is governed by $F(Q^2/S)$, the probability function of finding the above parton-antiparton pair with fractional momenta X_1 and X_2.

Thus, the dilepton spectrum from hadron-hadron collisions in the deep scattering region is given by:

$$\frac{d\sigma}{dQ^2} = \frac{4\pi\alpha^2}{3Q^4} F(Q^2/s) \qquad (20)$$

where

$$F(Q^2/s) \longleftrightarrow \{F_2(x_1, \text{hadron}_1 \text{ parton}); F_2(x_2, \text{hadron}_2 \text{ antiparton})\}$$

is the overlap of two structure functions.

We propose to test the scaling behavior predicted by equation (20) for hadron-hadron collisions. Up until the present, the scaling in reactions (17) or (18) has not been established. At NAL, it will be possible to test in a straightforward manner the central idea of hadron constituent theories, only if experiments are made, at the same time, on reactions (11-12) with pions (this proposal) and on reaction (17) with protons (the proposal of E-70). Scaling can be established or new phenomena discovered

by examining the behavior of the functions $F_{\pi N}(Q^2/s)$ and $F_{pN}(Q^2/s)$

Briefly, these functions can be measured by the observed lepton pair spectra from both experiments, using eq.(20).However, more than this can be made available by the proposed comparison of results from pion and proton beam experiments. A remarkable and instructive test is made available by measuring the parton distribution functions of pions and nucleons. The test is made by observing the folded parton distribution among the π-N and p-N collisions. The double differential cross sections as a function of dilepton mass and their momentum transfer provide the following measurement:

$$\left.\begin{aligned} (Q^2 - t)Q^4 \frac{d^2\sigma}{dQ^2 dt} &= \frac{4\pi\alpha^2}{3} \sum_a \frac{F_{2a}(x_1,h_1)F_{2\bar{a}}(x_2,h_2)}{\lambda_1^2 \lambda_2^2} \quad \lambda_{12}^2 \\ t &= (Q - P_1)^2 \simeq Q^2 - x_2 s \\ Q^2 = M_{\ell'\ell}^2 &= 2E_+E_-[1 - \cos(\theta^+ + \theta^-)] \simeq x_1 x_2 s \end{aligned}\right\} \quad (21)$$

whereby, the scaling variable Q^2/s and the fractional momentum transfer between lepton pairs and incident particle, t/s, define the fractional momentum of partons and antipartons, X_1 and X_2. Therefore, the measured quantity on the left hand side of Eq.(21)can be examined as a function of X_1 and X_2 for the case of π-N and p-N collisions. (We can only wish that there would be sufficient antiproton intensity in our beam to allow us to measure in a limited kinematical region, the very exciting reactions:

$$\bar{p} - N \rightarrow e^+e^- + \text{anything} \quad (22)$$

$$\bar{p} - N \rightarrow \mu^+\mu^- + \text{anything} \quad (23)$$

These would make unnecessary the assumption[6] that the parton distribution in protons is the same as the antiparton distribution in antiprotons.

We would be able to measure these fundamental distributions and test the assumptions.)

In the above tests, we propose to investigate the symmetry property of π - N collisions producing large mass lepton pairs. The measured double differential cross sections of Eq.(21) must be asymmetrical under the interchange of X_1 with X_2 because there should certainly be more antipartons in the π - N system as compared with the p - N initial state. By the same reasoning, we expect to find higher cross sections for the pion induced reactions (11-12) than the proton reaction (17), especially at large Q^2/s values. This would also be helpful in compensating for the difference of pion and proton beam intensities at NAL, although our experiment is designed to handle this situation adequately, independent of this expectation.

2. Search for Intermediate Vector Bosons, Lee-Wick Heavy Photons and Heavy Leptons in Meson-Nucleon Collisions.

We propose to search for the production of intermediate vector bosons $W_1^{+,-}$, heavy leptons $L^{+,-,o}$, and Lee-Wick heavy photons B^o, in pion-nucleon collisions. The heavy leptons can be produced in pairs by the electromagnetic interaction in deep π - N collisions.

Reactions (11), (12) and (13) are the best candidates for the production of heavy leptons in pairs:

$$\begin{aligned} \pi^- N &\rightarrow L^+ L^- + \text{anything} \\ L^+ &\rightarrow e^+ \bar{\nu}_L \nu_e \,;\; \mu^+ \bar{\nu}_L \nu_\mu \\ L^- &\rightarrow e^- \nu_L \bar{\nu}_e \,;\; \mu^- \nu_L \bar{\nu}_\mu \end{aligned} \qquad (24)$$

Theoretical calculations of the various decay branching ratios of heavy leptons show that the above decay modes are prominant. Typically, the decay modes with electrons and muons constitute two thirds of the total decay rate. The branching ratios of heavy leptons are calculated as a function of assumed lepton mass values. This is given in Table I, from one calculation[7], and also from an independent calculation[8], in Fig. 3. The transverse momentum spectra of large angle lepton pairs $e^{\pm}$, $\mu^{\mp}$ will be examined especially to search for structure in the single spectrum of $e^{\pm}$ or $\mu^{\pm}$. The transverse momentum spectrum of these $e^{\pm}$ $\mu^{\mp}$ pairs in each case, will also be examined to ascertain that these pairs are not correlated. The observation of correlated $e^{\pm}$ $\mu^{\mp}$ pairs is a clear signal for the production of a neutral heavy lepton[8], decaying in the mode:

$$E^{o} \rightarrow e^{+}\mu^{-}\bar{\nu}_{\mu}$$
$$\bar{E}^{o} \rightarrow e^{-}\mu^{+}\nu_{\mu} \qquad (25)$$

We propose to search for structure in the lepton pair mass spectra of reactions (11-12). Correlated $e^{+}e^{-}$ and $\mu^{+}\mu^{-}$ lepton pairs from the decay of Lee-Wick heavy photons[9] would exhibit prominant structure in the dilepton effective mass spectra. These peaks would be found over the continuum of the dilepton mass distributions; due to the electromagnetic interaction processes, producing

$$\pi^{-}N \rightarrow B^{o} + \text{anything}$$
$$B^{o} \rightarrow e^{+}e^{-};\ \mu^{+}\mu^{-} \qquad (26)$$

in the form of "heavy photon bremsstrahlung".

We plan to search for the production of intermediate vector bosons produced in deep π - N collisions via the semi-weak interaction processes.

TABLE I

Partial and total decay rates of l for various values of M_l. Decay rate $(10^{10}\ \text{sec}^{-1}) = (\Gamma/\hbar) = 1/\tau$.

M_l (GeV)	0.6	0.8	0.938	1.2	1.8	3.0	6.0
Decay mode							
$l \to \nu_l + \nu_e + e$	0.266	1.12	2.46	8.5	64.6	831	26 600
$\nu_l + \nu_\mu + \mu$	0.2	0.96	2.21	7.97	63	823	26 533
$\pi + \nu_l$	1.02	2.57	4.17	9.0	30	143	1145
$K + \nu_l$	0.0092	0.09	0.2	0.55	2.3	11.7	98
$\rho + \nu_l$	0	0.21	3.8	19	96	486	3900
$K^* + \nu_l$	0	0	0.03	0.96	6.3	33	280
$A_1 + \nu_l$	0	0	0	0.6	33.7	364	1550
$Q + \nu_l$	0	0	0	0	0.17	15.2	133
ν_l + hadron continuum	0	0	0	0.5	27	737	25 900
$l \to \nu$ + hadrons	1.03	2.87	8.2	29.6	195	1790	33 006
Total rate	1.5	4.95	12.9	46.1	323	3444	85 539
Decay length in cm at $E_l = 5$ GeV	16.5	3.73	1.2	0.26	0.024	...	...
Decay length in cm at $E_l = 50$ GeV	167	37.7	12.2	2.7	0.257	0.0145	...

2130A4

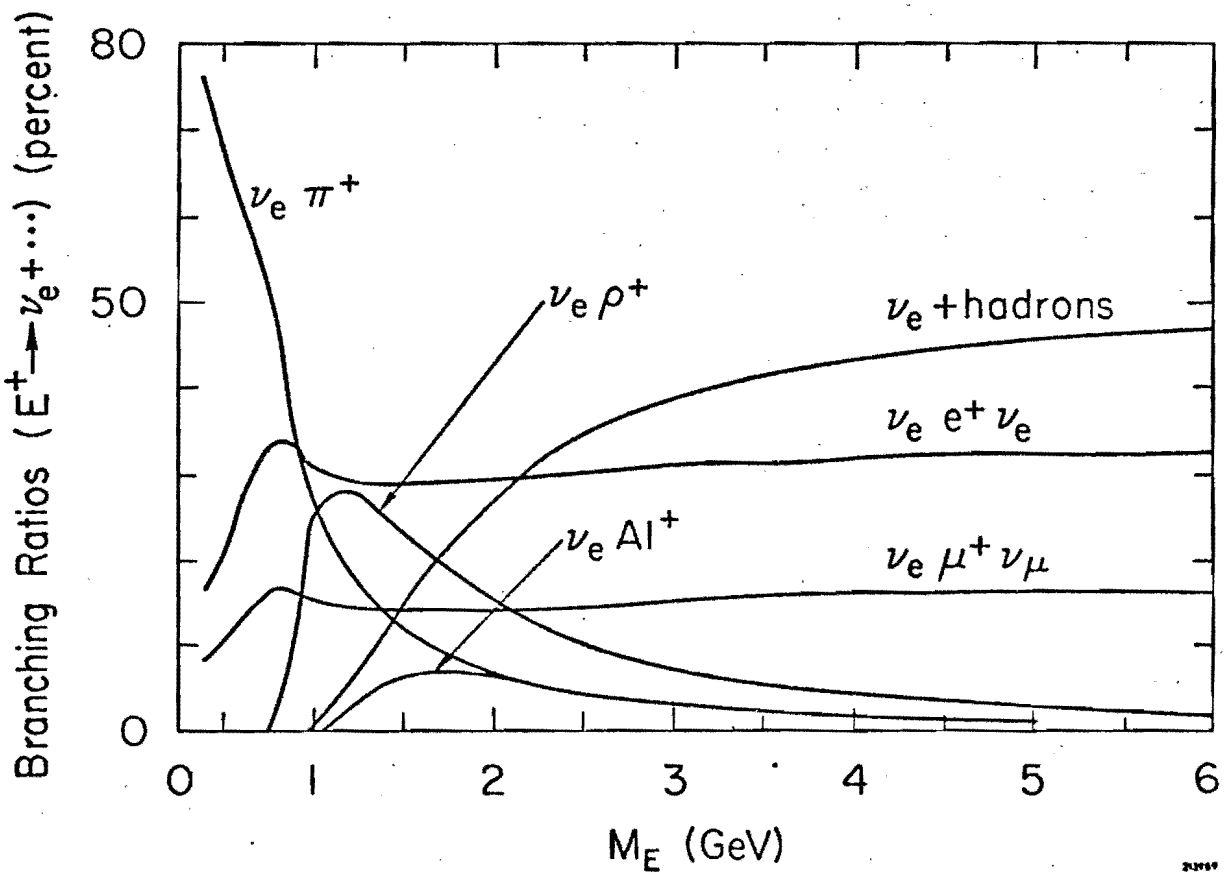

Figure 3

$$\pi^- N \rightarrow W_1^{\pm} + \text{anything}$$

$$W_1^+ \rightarrow e^+ \nu_e \; ; \; \mu^+ \nu_\mu \qquad (27)$$

$$W_1^- \rightarrow e^- \bar{\nu}_e \; ; \; \mu^- \bar{\nu}_\mu$$

This reaction would produce single leptons having anomalously large transverse momentum values. The transverse momentum spectra of final state single leptons, ($e^{\pm}$, $\mu^{\pm}$) would show a sharp upper cutoff, at a value corresponding to the mass M_W, at $P_\perp$ ($e^{\pm}$ or $\mu^{\pm}$) $\approx M_W/2$.

It is in this important search where the use of pion beams could excel over protons. If indeed, constituents of hadrons do exhibit also point Fermi interactions, the production of W's is enhanced further with π - N collisions than in p - N collisions. This is because pions have more antipartons which carry also a higher fraction x of the available momenta. In pions, it is expected[10] that the fractional momentum distribution of partons is $\sim (1 - x)$, whereas in protons these are distributed like $(1 - x)^3$ near $x \sim 1$. This is indicated by the behavior of nucleon structure functions measured from deep e - p collisions. In the case of $(1 - x)$ parton distribution it is demonstrated[11] that the point Fermi interactions of parton-antiparton pairs,

$$q\bar{q} \rightarrow \ell\nu$$

is enhanced by two orders of magnitude, as compared to the case of parton distribution in protons. Therefore, we could expect to find that the yield of reaction (27) is two orders of magnitude higher than the equivalent semi-leptonic interaction yield from p - N collisions:

$$p + N \rightarrow W_1^{\pm} + \text{anything} \qquad (28)$$

In Fig. 4 the semi-leptonic interaction diagram is depicted, characterizing the π - N collisions of reaction (27). Also shown on this figure is the production cross section of proton initiated collisions, as a function of the assumed mass of intermediate vector bosons. This calculation[1] is based on the point Fermi interaction of partons in reaction (28). Other calculations[12, 13] give similar results, where also the production cross sections of B^o and heavy leptons are presented, always for proton initiated collisions.

We also propose to search for structure in the mass combination of $(e^{\pm} \gamma)$ and $(\mu^{\pm} \gamma)$ from the coincidence measurements of reactions (15) and (16). Structure could be found in these lepton-gamma-ray pair mass distributions due to the production of heavy excited leptons.

In Table II we summarize the search program of this experiment. We give the available mass limits, cross section estimates at these mass limits, the additional enhancement factor of pion initiated collisions which should multiply the given cross sections, and the various combinations in singles or in pairs. We show that the experimental sensitivity to produce any 100 sought events is $\sigma \cdot B = 10^{-36} cm^2$; so that, the limiting sensitivity in our experiment, in case of negative result, is $\sim 10^{-38}$ cm^2.

We stress that between our pion beam experiment and the associated electron beam experiment proposals, a viable, advantageous and imaginative search program is envisaged at NAL. This program is designed to take advantage of the hadronic, electromagnetic and semi-weak interaction processes occuring in π - N and e - N deep scattering collisions, more in one than in the other as the case may be, to produce the B^o, $W_1^{\pm}$, $L^{\pm}$, E^o and E^* massive

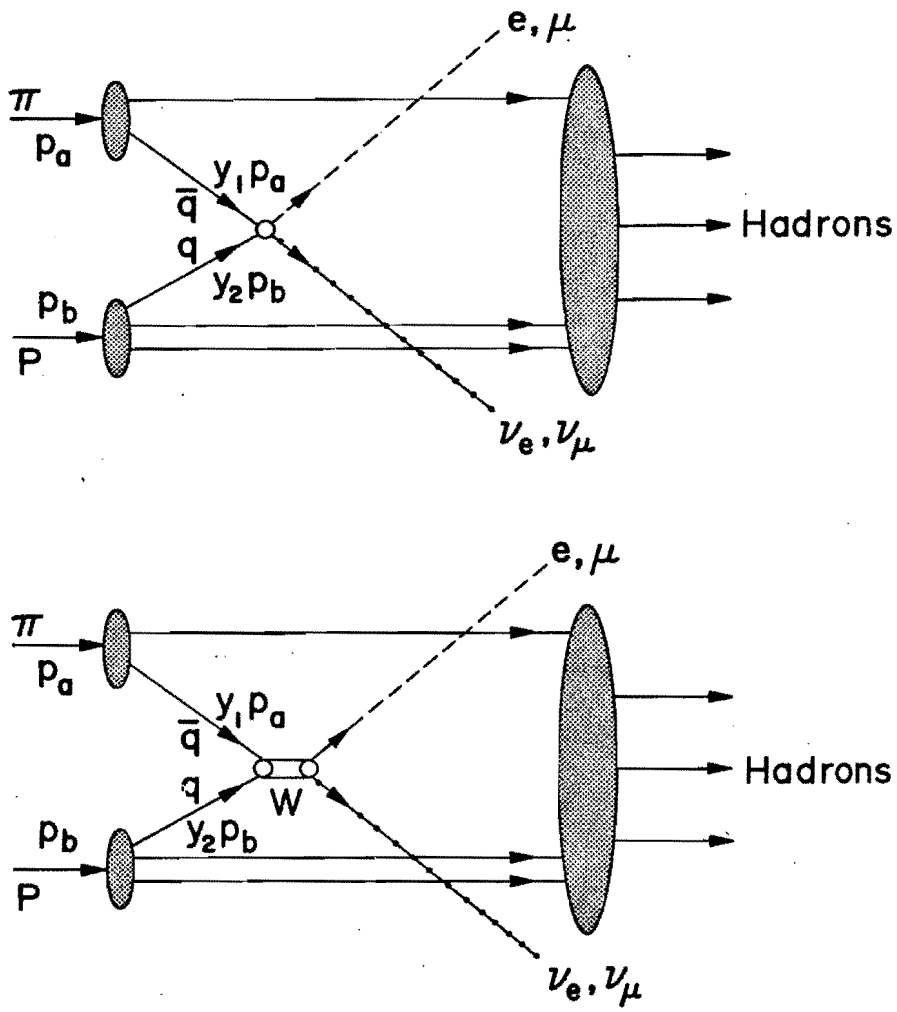
e, μ
π
p_a
y_1 p_a
q̄
q
y_2 p_b
p_b
P
Hadrons
ν_e, ν_μ
e, μ
π
p_a
y_1 p_a
q̄
q
W
y_2 p_b
p_b
P
Hadrons
ν_e, ν_μ

Figure 4

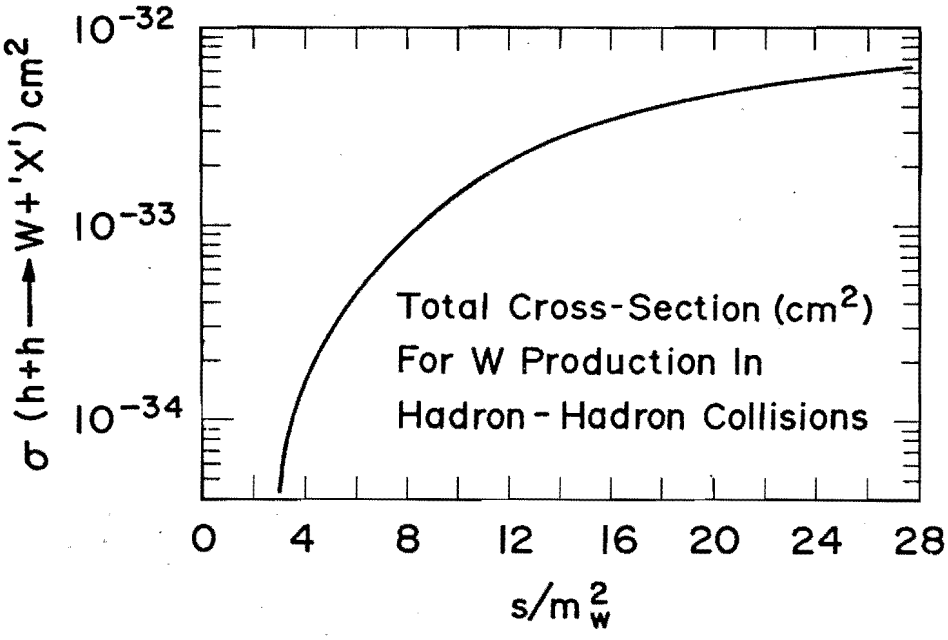
σ (h+h → W+'X') cm²
10⁻³²
10⁻³³
10⁻³⁴
Total Cross-Section (cm²)
For W Production In
Hadron - Hadron Collisions
0
4
8
12
16
20
24
28
s/m²_W

TABLE II

PRODUCTION OF MASSIVE OBJECTS IN 150-300 GeV π^-N COLLISIONS AT NAL

MASSIVE OBJECT	PROPOSED SEARCH SAMPLE	ESTIMATED σ P-P COLLISIONS AT MASS LIMITS	ESTIMATED σ ENHANCEMENT FACTOR FOR π^-- N COLLISIONS	MASS LIMITS (GeV)
B^o	e^+e^-, $\mu^+\mu^-$ mass of pairs	$\sim 10^{-33}$	5-10	21
$W^{\pm}$	$e^{\pm}$, $\mu^{\pm}$ singles large $P_\perp$	$\sim 10^{-34}$	50-100	17
L^+L^-	$e^{\pm}\mu^{\mp}$ uncorrelated pairs, large $P_\perp$	$\sim 10^{-35}$	5-10	8
$E^o(\bar{E}^o)$	$e^{\pm}\mu^{\mp}$ correlated pairs	$\sim 10^{-35}$	5-10	8
$E^{*\pm}$	$e^{\pm}\gamma$ mass of pairs	$\sim 10^{-35}$	5-10	8
$M^{*\pm}$	$\mu^{\pm}\gamma$ mass of pairs	$\sim 10^{-35}$	5-10	8
Time-like Photons	e^+e^-, $\mu^+\mu^-$ mass of pairs (continuum)	$\sim 10^{-36}$	5-10	20

Experimental sensitivity for $10^9\pi$/pulse, in a given search of 100 hr (10^5 pulses) with 10% beam interacting in target, 20% geometrical efficiency and for the observation of 100 sought events:

$$100 \text{ events} = (\sigma \cdot B) \times 10^9 \times 0.10 \times 10^5 \times 0.20/(20 \times 10^{-27})$$

$$\sigma \cdot B = 10^{-36} \text{cm}^2. \quad \text{(Production cross section x Branching Ratio)}$$

objects. If the masses are within reach of NAL energies then we are confident of positive results. Otherwise, our experiments, and especially the electron beam experiment, are designed to provide meaningful and reliable mass limits. The information arrived at by these experiments is essential and timely in the planning and design of new[14] high energy physics installations.

3. Study of Forward Produced Multi-Gamma-Ray Final States from π - N Collisions.

Several unique processes are involved in the production of multi-gamma-ray final states. These are from π - N hadronic collisions at relatively small transverse momenta. The physics interest of forward produced multi-gamma-ray reactions is presented in great detail in our original proposal 164-I. We refer the reader to this document for further details. Briefly, we propose to make a systematic study at NAL energies of the exclusive reactions

$$\pi^- + N \rightarrow N + n\gamma; \quad n = 1, 2, 3 \text{ and } 4 \qquad (29)$$

and the inclusive

$$\pi^- + N \rightarrow n\gamma + \text{anything} . \qquad (30)$$

We will search for the production of new massive bosons, up to 5 GeV mass values, and observe the multi-gamma-ray mass spectra in several well defined mass combinations. In general, the quality of this new work will compare directly with the physics obtained from a large acceptance multi-charged-particle spectrometer system, such as the MPS at BNL and the OMEGA at CERN. The reactions in (29-30) have not yet been explored with sufficient care and accuracy. This is because up until recently, difficulties existed with producing multi-gamma-ray detectors. We have proposed a way

to overcome this restriction by devising a new multi-gamma-ray spectrometer system having the following properties: 1) large acceptance, 2) excellent energy resolution in the measurement of total energy of a multi-gamma-ray state, 3) good space resolution in the measurement of individual gamma-ray coordinates, 4) a gamma-ray pair resolution limited only by the natural width of high energy showers ($\sim$ 3 cm), 5) coarse resolution in the measurement of individual gamma-ray energies and 6) a detector data acquisition rate limited only by the electronics and on-line computer system. We have shown that with the above properties (2-4), multi-gamma-ray mass combinations are defined with an accuracy of $\Delta M/M \lesssim 2\%$. The momentum transfer resolution is about 5 times better than in any other similar experiment or proposal known to us.

Recently, two related experiments were made. One studied the reaction in (29) at CERN energies[15] and the other was concerned with $K^o \to \pi^o\pi^o$ measurements[16] also at CERN. At NAL energies our method compares favorably with both of these cases.

Finally, we discuss a new theoretical development which makes the study of:

$$\pi^- N \to \gamma + \text{hadrons} \qquad (31)$$

at high energies, and at $k_\perp^\gamma < 20$ MeV, a very attractive source of new information ($k_\perp^\gamma$ is the transverse momentum of gamma-rays). In Fig. 5 the equivalent reaction from p - p collisions measured at the ISR[17] is shown. Basically, the process is examined[18] as being the bremsstrahlung by hadrons, producing low transverse momentum energetic gamma rays. It is found[18a] that this process provides directly a measure of the average charge multiplicity in hadron-hadron collisions.

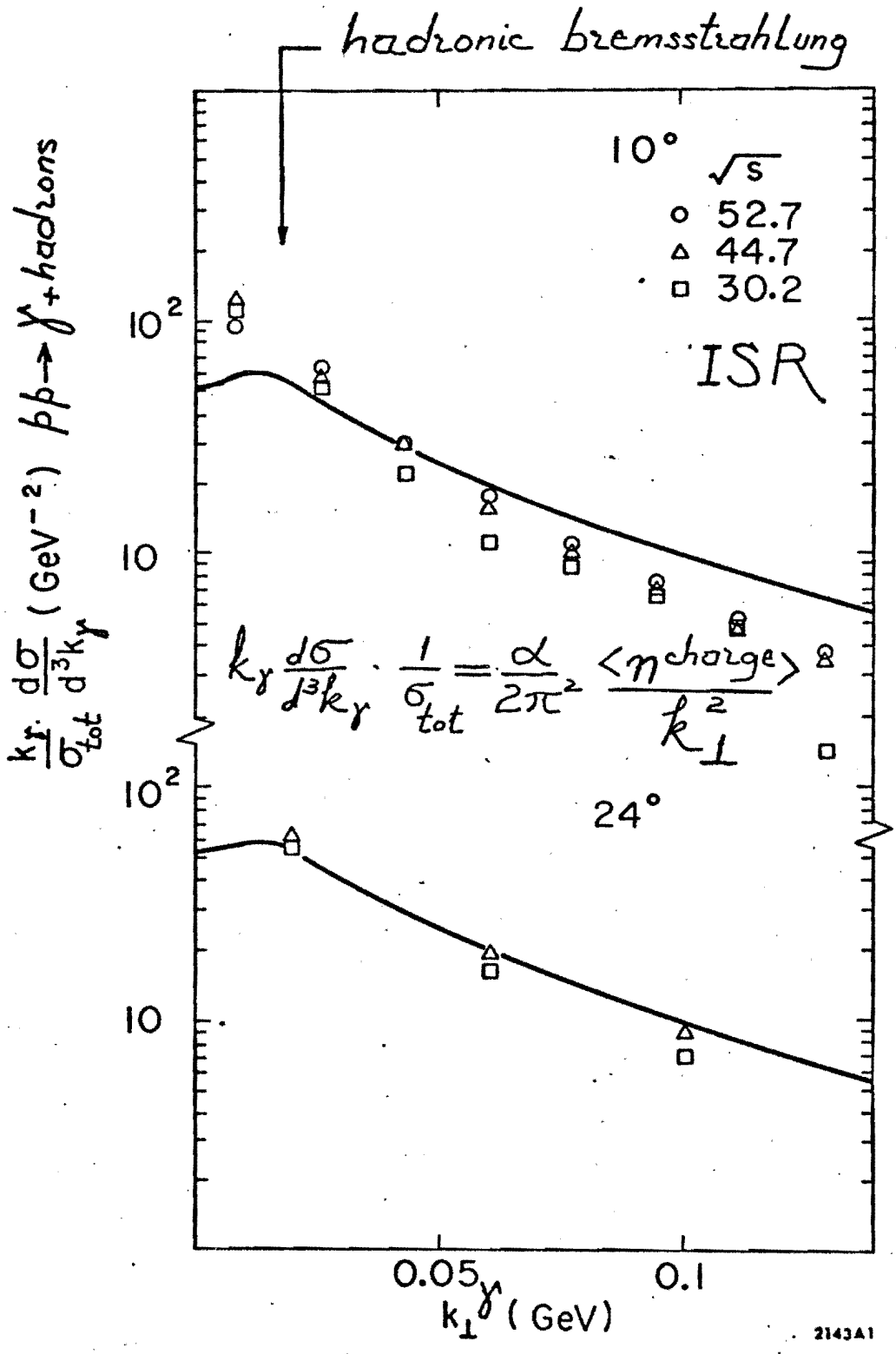
hadronic bremsstrahlung
10°
√s
52.7
44.7
30.2
ISR
$\frac{k_\gamma}{\sigma_{tot}} \frac{d\sigma}{d^3k_\gamma}$ (GeV^{-2}) $pp \to \gamma$ + hadrons
$k_\gamma \frac{d\sigma}{d^3k_\gamma} \cdot \frac{1}{\sigma_{tot}} = \frac{\alpha}{2\pi^2} \frac{\langle n^{charge} \rangle}{k_\perp^2}$
10^2
10
10^2
24°
10
0.05
0.1
$k_\perp^\gamma$ (GeV)
2143A1

Figure 5

Thus, we propose to measure the average charge multiplicity $\langle n_{ch} \rangle$ in π - N collisions, using this method and the measurements of reaction (31). We will compare our determination of $\langle n_{ch} \rangle$ with say, bubble chamber measurements at NAL. The difference between both measurements is very significant and would be due to charged pair correlations in multiplicities.

III. HIGH ENERGY PION BEAM AT NAL

We have designed[20] a high quality 300 GeV electron beam for NAL. Initially this design work was begun for the benefit of our associated electron experiment. Details of the beam design and descriptions of the qualities are presented in Appendix I of our electron proposal.

It is clear that this beam can also be used as an excellent 300 GeV pion facility at NAL. It will provide a beam of pions at NAL which is higher in energy and intensity than any other presently installed secondary beam. The changeover from electrons to pions and back is performed easily. A lead radiator is removed and a set of initial steering magnets are turned off. However, a different proton beam dump is required.

The beam delivered at the experimental target is very clean. A final spot size of $\pm$ 2 mm is obtained without any loss in intensities. We have calculated the yield of negative pions using a multiperipheral model[21] of p-p collisions. The model successfully fits with yield measurements at BNL and CERN. In Fig. 6, the result of this calculation is displayed for the cases of 400 GeV and 500 GeV incident protons. The yield of pions in this beam is high. This is due to the large acceptance of the beam (9.5 μst % Δ p/p FW, and Δ p/p $\tilde{-} \pm$ 2%) and the high energies

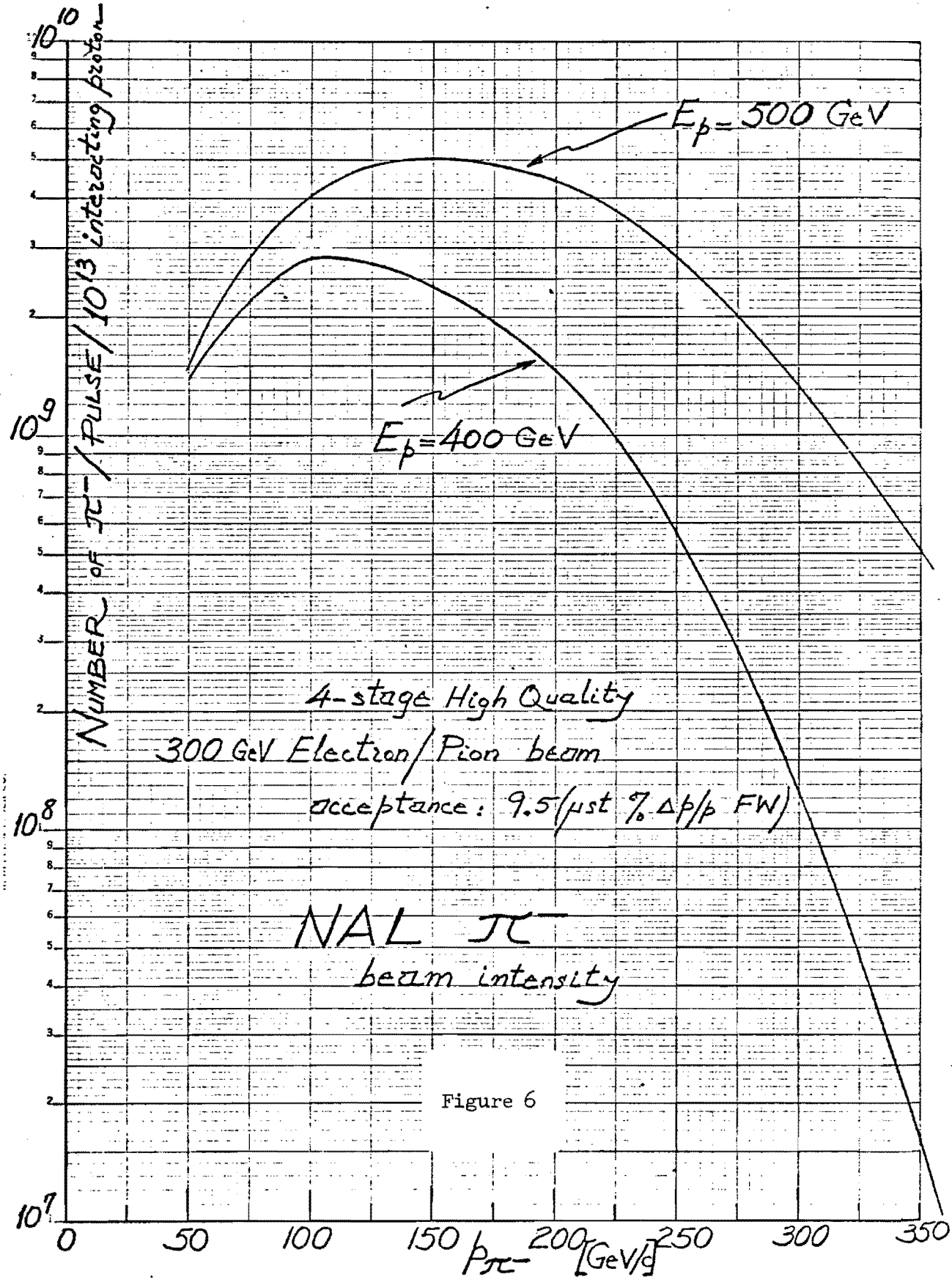
E_p = 500 GeV
E_p = 400 GeV
4-stage High Quality
300 GeV Electron/Pion beam
acceptance: 9.5 (μst % Δp/p FW)
NAL π⁻
beam intensity
NUMBER OF π⁻/PULSE/10¹³ interacting proton
10^{10}
10^{9}
10^{8}
10^{7}
0
50
100
150
200
250
300
350
P_{π^-} [GeV/c]

Figure 6

of the incident protons. At the Proton Laboratory, 400 - 500 GeV external proton beams can be made available. Therefore, we propose to use this beam for pions in the energy range of 150 - 300 GeV and intensities of 10^8 - 10^9 π / 10^{12} protons. There may be other reasons at this time that restrict the use or construction of this beam as a 300 GeV electron/pion facility. We are not aware of these considerations. Should this be the case, we propose to use initially for this experiment, the 2.5 mrad beam branch at the Meson Laboratory and to start the experiment at lower energies and intensities: 40 - 140 GeV, 10^5 - 10^6 π / 10^{12} protons.

IV. EXPERIMENTAL METHOD

1. 20 kgauss Superconducting Dipole Magnet

For both our proposed pion and electron experiments at NAL, a 20 kgauss analyzing dipole magnet is required. The magnet will have a length of 15 ft and a useful aperture of 3 ft in width and 1 ft gap. The analyzing magnet discussed in our original proposal No. 164 has now been redesigned and modified so that it will have superconducting coils. Following our feasibility studies we present a preliminary design of this magnet. An equivalent 18 kgauss magnet with conventional copper coils will consume 1.07 Mwatt power and is estimated to cost $ 180 K. The cost estimate of this superconducting 20 kgauss magnet is about $ 150 K, exclusive of the cryogenic refrigerator system.

Among recent advances in the manufacture of superconductors, a search was made to select a superconductor configuration providing reliable and safe operation. Presently, we favor the following available superconductor: a continuous copper ribbon, 1/16" thick and 2" wide with

embeded Niobium-Tin superconducting strips. This material conducts adequately 1000 A in a magnet at 30 kgauss.

The dipole magnet design is shown in Fig. 7. Superconducting coils with mechanical supporting ribs are shown inside a helium dewar. This is a 500 liter dewar and is heat shielded by layers of super-insulation, a nitrogen shield, again super-insulation and vacuum. The dewar fits inside a window frame iron magnet. The total amper-turns are 722,000 AT. A current density of 20,000 A/cm^2 is made available in a coil cross section area of 50 cm^2. In each turn a current of 1000 A will be conducted, for a total of 722 turns in each coil. The weight of this magnet is 140 tons. The magnet will be built in sections which will make it easier to assemble or dismantle for shipment to NAL. For the final coil configuration we intend to make calculations with available computer programs, to gradate the current density in the coils and thus achieve a high magnetic field uniformity inside the useful aperture.

We propose to build this magnet for NAL, using our own facilities at HEPL. We have the manpower and equipment to complete this important task. We are presently building an iron magnet approximately eight times as massive as the one described above.

2. Experimental Configurations and Acceptances of the Spectrometer System.

The makeup of our spectrometer system is simple and modular. Briefly, the central idea is this. With a pion or electron beam, a target and a beam monitor, an analyzing magnet is used together with two large acceptance spectrometer arms to do coincidence measurements. One of these arms is always used to trigger candidate events. This arm will make measurements in singles, on inclusive reactions. The second arm is placed

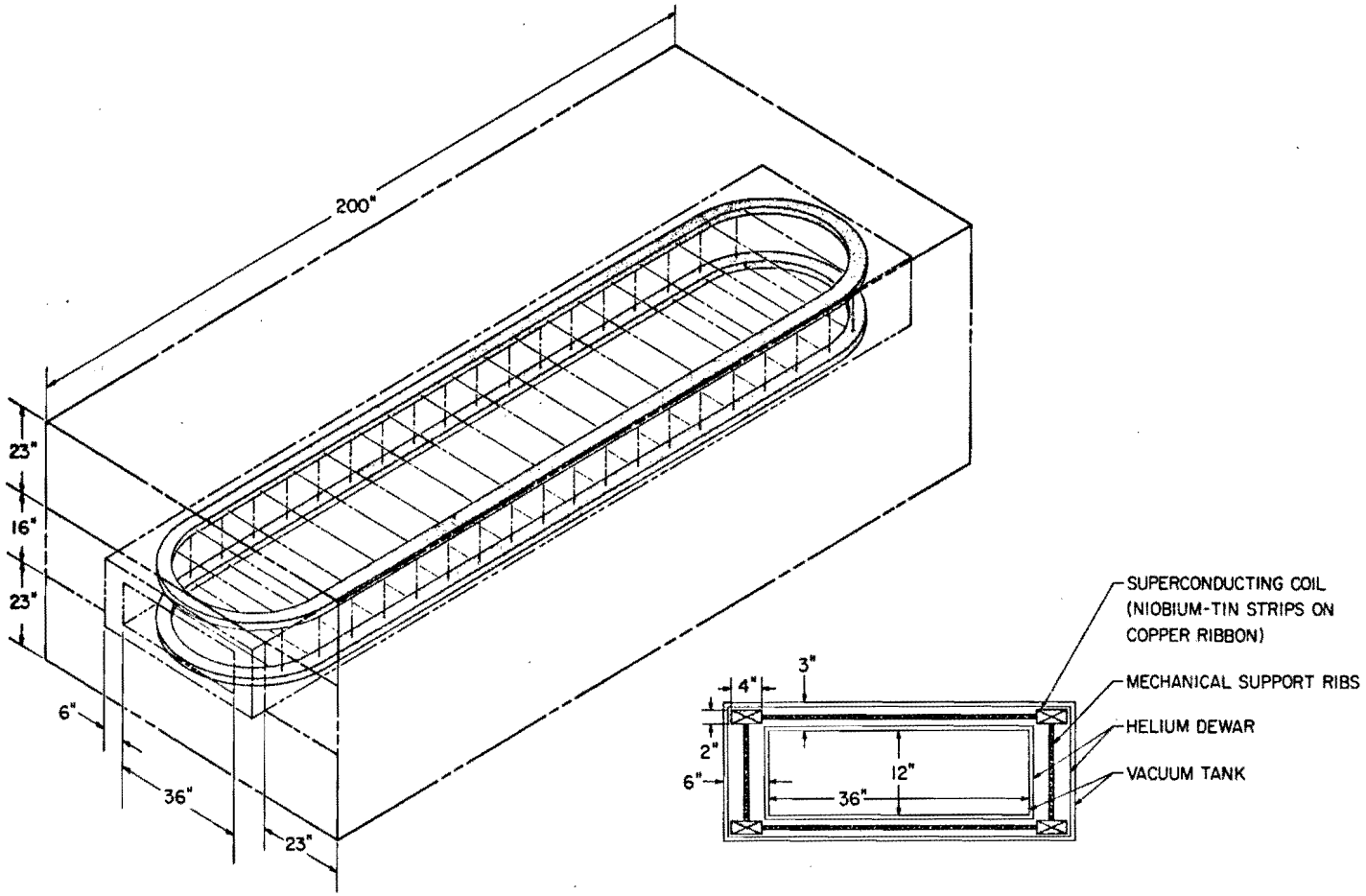

B = 20 kG
J = 20,000 A/cm^2
SC COIL = 650,000 A-TURNS
Fe RETURN = 72,000 A-TURNS
WEIGHT = 140 TON

20 kG SUPERCONDUCTING DIPOLE MAGNET
(15ft x 3ft x 1ft)

Figure 7

essentially at three different locations to provide coincidence measurements selectively.

Using these as building blocks, we have devised specific spectrometer configurations which favor in each case the observation of a few processes among several ongoing reactions. In our original proposal 164, the design principles, the function of individual components and the qualities of spectrometer modules were described in detail. We have modified the composition of spectrometer modules to include muon identifiers. Thus, a modified and improved spectrometer is now obtained which has the capability of observing multi-gamma-ray or multi-lepton final states.

In Fig. 8 the first configuration is shown. This is designed for the purpose of observing the processes mentioned therein. In this and other configurations, the experimental target is placed inside the magnet. It is desired 1) to achieve a large acceptance in production angles and in momenta and also 2) to provide good resolution in the measurements of angles and momenta. These economical and efficient spectrometer features are made possible only by having an incident beam spot size of dimensions no greater than $\pm$ 2 mm. This spot size quality is achieved with the beam in our design. In the bending plane, the transverse coordinate of track origins is anchored by the beam spot size definition. Three other coordinates are measured on charged particle tracks by multiwire proportional chambers. The orbit of tracks is defined with a long lever arm, as shown in this figure.

In Configuration (I) the beam line and target position are displaced vertically inside the magnet (for example, the magnet is lowered by about 6 inches). To observe efficiently the production of large angle and high momentum particles, the spectrometer module is placed in the forward direction,

CONFIGURATION I

DESIGNED FOR WIDE ANGLE PRODUCTION OF SINGLE LEPTONS AND/OR SINGLE PHOTONS

$\pi^- N \rightarrow e^{\pm} +$ HADRONS

$\pi^- N \rightarrow \mu^{\pm} +$ HADRONS

$\pi^- N \rightarrow \gamma +$ HADRONS

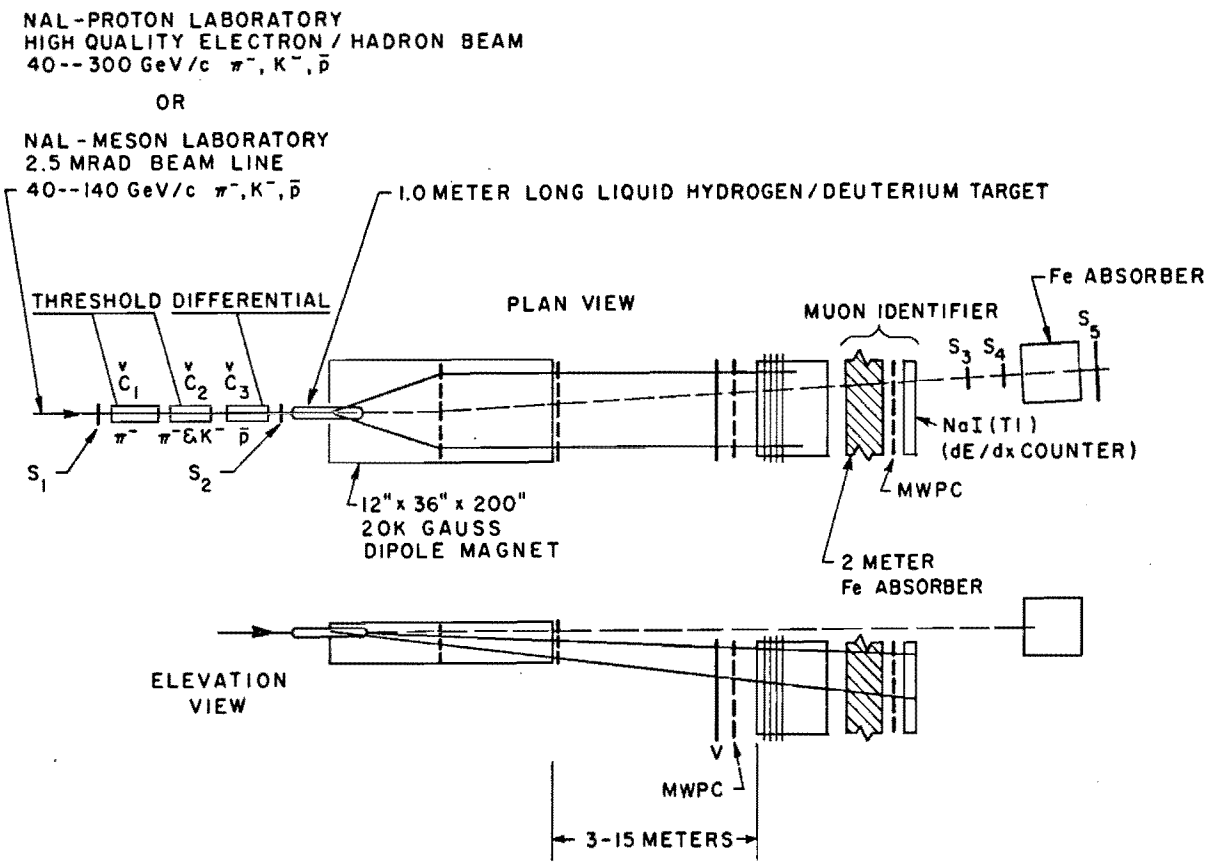

SCHEMATIC EXPERIMENTAL SETUP

(NOT TO SCALE)

Figure 8

below beam line. Thus, the observation of high energy and large angle emerging $e^{\pm}$, $\mu^{\pm}$, and γ, singles is enhanced; and low energy or forward produced particles are not seen by the forward spectrometer arm. These features are demonstrated in Fig. 8 and seen in Table III.

We have used a Monte Carlo program to map out extensively the acceptance regions of the spectrometer system and to define those regions which are of interest to the physics considerations. In terms of the correlated quantities p and θ (momentum and production angle of produced particles) the acceptance calculations are given in bins of p and θ. The percentage of azimuthal angle accepted in a cell defined by Δp and $\Delta\theta$ is stated. This and the following tables are generated for the case of an incident pion beam of 150 GeV/c.

In Table III (a) the acceptance of the forward spectrometer is depicted for positively charged particles, emerging at large angles and with high energies from the target. Table III (b) is the same for negatively charged particles. It is seen that both positively and negatively charged particles, emerging only at large angles and also with high energies, are accepted symmetrically and equally as well. The Monte Carlo calculation of Table III is made with the target placed just at the entrance of the analyzing magnet. The forward spectrometer is assumed to be set 5 meters away from the magnet exit. It is clear that larger angles and higher momenta can be accepted by moving the target position forward and/or moving the forward spectrometer arm further away.

In Table IV the results of Monte Carlo acceptance calculations are shown for two other spectrometer module locations. In these cases, the beam line and target position are centered vertically inside the analyzing magnet. In Table IV (a) the target is from the entrance side 2 meters inside the

PHI/2PI IN PERCENT
ACCEPTANCE OF MAGNET/NA(TL) CRYSTAL/MWPC COMBINATION.

MOMENTUM (GEV/C)	SCATTERING ANGLE THETA (MRAD) 5.2	10.4	15.6	20.8	26.0	31.3	36.5	41.7	46.9	52.1	57.3	62.5	67.7	72.9	78.1	83.3	88.6	93.8	99.0	104.2
11.0	0	0	0	0	0	0	0	0	0	0	0	0	0	0	0	0	0	0	0	0
21.0	0	0	0	0	0	0	0	0	0	0	0	0	0	0	0	0	0	1	0	0
31.0	0	0	0	0	0	0	0	0	0	0	4	0	7	3	10	4	7	9	0	1
41.0	0	0	0	0	0	0	0	1	14	4	22	7	16	7	13	6	8	6	0	1
51.0	0	0	0	0	0	3	15	12	17	12	24	7	14	6	11	4	3	3	0	0
61.0	0	0	0	0	6	14	15	23	13	20	24	7	16	1	10	2	0	0	0	0
71.0	0	0	0	6	13	25	15	26	14	26	20	6	16	0	7	0	0	0	0	0
81.0	0	0	0	8	20	30	15	34	18	21	18	4	17	0	2	0	0	0	0	0
91.0	0	0	0	14	21	30	17	34	13	26	13	2	10	0	0	0	0	0	0	0
101.0	0	0	8	21	20	34	19	40	15	27	15	2	10	0	0	0	0	0	0	0
111.0	0	0	13	22	24	30	20	35	13	26	11	3	9	0	0	0	0	0	0	0
121.0	0	0	19	26	30	26	21	33	14	34	9	7	5	0	0	0	0	0	0	0
131.0	0	3	25	22	29	27	22	37	14	33	8	6	4	0	0	0	0	0	0	0
141.0	0	4	28	22	33	25	28	27	17	28	5	9	3	0	0	0	0	0	0	0
151.0	0	6	25	22	34	21	31	25	24	27	4	9	1	0	0	0	0	0	0	0

INITIAL EVENTS=100000 FINAL EVENTS= 7769

0.0	5.000	5.000	0.0	0.250	0.050	0.457	0.457			
1.000	0.325	0.0	0.0	151.000	1.000	0.0	20.000			
0.09140	0.09140	0.09140	0.05000	0.05000	0.01000	0.01987	0.0	0.10418	0.15901	0.0 -0.3

Table III

(b)

PHI/2PI IN PERCENT
ACCEPTANCE OF MAGNET/NA(TL) CRYSTAL/MWPC COMBINATION.

MOMENTUM (GEV/C)	SCATTERING ANGLE THETA (MRAD) 5.2	10.4	15.6	20.8	26.0	31.3	36.5	41.7	46.9	52.1	57.3	62.5	67.7	72.9	78.1	83.3	88.6	93.8	99.0	104.2
11.0	0	0	0	0	0	0	0	0	0	0	0	0	0	0	0	0	0	0	0	0
21.0	0	0	0	0	0	0	0	0	0	0	0	0	0	0	0	0	0	1	1	0
31.0	0	0	0	0	0	0	0	0	0	0	4	1	5	9	3	15	0	7	0	0
41.0	0	0	0	0	0	0	0	2	12	3	23	9	16	13	5	14	0	12	0	0
51.0	0	0	0	0	0	6	5	14	17	16	23	7	19	7	9	5	0	5	0	0
61.0	0	0	0	0	5	21	21	18	23	16	22	7	15	2	9	0	0	0	0	0
71.0	0	0	0	0	14	19	19	15	29	17	17	9	14	0	7	0	0	0	0	0
81.0	0	0	0	5	13	31	19	29	25	16	10	14	9	0	4	0	0	0	0	0
91.0	0	0	4	14	15	36	15	33	15	18	7	19	3	2	0	0	0	0	0	0
101.0	0	0	7	25	19	33	15	37	17	28	3	15	0	1	0	0	0	0	0	0
111.0	0	0	19	19	24	32	23	33	17	30	8	14	0	1	0	0	0	0	0	0
121.0	0	0	19	21	28	24	28	29	19	28	13	10	0	1	0	0	0	0	0	0
131.0	0	1	23	17	37	23	29	24	23	24	14	3	0	2	0	0	0	0	0	0
141.0	0	0	19	23	33	18	31	24	25	20	15	2	2	0	0	0	0	0	0	0
151.0	0	1	18	24	36	19	35	17	30	15	14	0	1	0	0	0	0	0	0	0

INITIAL EVENTS=100000 FINAL EVENTS= 7687

0.0	5.000	5.000	0.0	0.250	0.050	0.457	0.457			
1.000	0.325	0.0	0.0	151.000	-1.000	0.0	20.000			
0.09140	0.09140	0.09140	0.05000	0.05000	0.01000	0.01987	0.0	0.10418	0.15901	0.0 -0.3

PHI/2PI IN PERCENT
ACCEPTANCE OF MAGNET/NAI(TL) CRYSTAL/MWPC COMBINATION.

MOMENTUM (GEV/C)	SCATTERING ANGLE THETA (MRAD) 8.0	16.0	24.0	32.1	40.1	48.1	56.1	64.1	72.1	80.2	88.2	96.2	104.2	112.2	120.2	128.3	136.3	144.3	152.3	160.3
11.0	7	5	9	7	7	6	9	8	10	9	7	8	7	4	5	3	4	1	3	0
21.0	100	99	94	87	87	83	48	22	7	6	2	0	0	0	0	0	0	0	0	0
31.0	100	100	99	92	75	57	38	30	22	15	1	0	0	0	0	0	0	0	0	0
41.0	100	97	80	62	55	43	38	33	21	24	10	8	0	0	0	0	0	0	0	0
51.0	98	71	50	48	47	41	40	30	24	25	20	18	2	0	0	0	0	0	0	0
61.0	76	57	49	32	46	35	31	28	28	23	18	18	3	0	0	0	0	0	0	0
71.0	38	42	50	33	46	33	28	35	26	20	21	15	8	8	0	0	0	0	0	0
81.0	12	32	38	30	39	30	27	31	26	20	18	22	12	11	0	0	0	0	0	0
91.0	5	35	37	36	33	35	32	33	25	24	21	18	15	11	0	0	0	0	0	0
101.0	0	25	31	33	32	36	27	29	25	21	18	16	18	11	0	0	0	0	0	0
111.0	0	15	33	30	30	33	25	31	24	24	18	15	14	11	0	0	0	0	0	0
121.0	0	11	32	29	30	32	29	27	23	19	24	17	16	9	0	0	0	0	0	0
131.0	0	9	29	30	30	29	31	28	27	23	20	17	17	10	7	0	0	0	0	0
141.0	0	8	32	25	34	27	34	29	18	21	19	16	17	7	10	0	0	0	0	0
151.0	0	8	31	23	33	27	40	29	25	19	17	18	13	9	13	0	0	0	0	0

INITIAL EVENTS=100000 FINAL EVENTS= 19819

0.0	3.000	3.000	0.0	0.150	0.150	0.457	0.457				
1.000	0.325	0.0	0.0	151.000	-1.000	0.0	20.000				
0.15233	0.15233	0.15233	0.05000	0.05000	0.05000	0.01192	0.0	0.16033	0.06364	0.45364	0.

Table IV

(b)

PHI/2PI IN PERCENT
ACCEPTANCE OF MAGNET/NAI(TL) CRYSTAL/MWPC COMBINATION.

MOMENTUM (GEV/C)	SCATTERING ANGLE THETA (MRAD) 4.8	9.6	14.4	19.2	24.0	28.9	33.7	38.5	43.3	48.1	52.9	57.7	62.5	67.3	72.1	77.0	81.8	86.6	91.4	96.2
-11.0	0	0	0	0	0	0	0	0	0	0	0	0	0	0	0	0	0	0	0	0
21.0	0	0	0	0	1	1	1	5	3	6	6	10	8	7	9	7	9	5	6	1
31.0	48	51	47	41	42	35	34	27	22	24	18	16	9	7	4	0	1	0	0	0
41.0	100	100	100	97	89	75	44	24	10	4	0	0	0	0	0	0	0	0	0	0
51.0	100	100	100	100	98	85	52	17	2	0	0	0	0	0	0	0	0	0	0	0
61.0	100	100	100	91	66	58	43	32	27	14	0	0	0	0	0	0	0	0	0	0
71.0	100	100	87	67	51	44	39	32	25	21	10	3	0	0	0	0	0	0	0	0
81.0	100	90	68	57	47	34	38	29	25	22	21	12	0	0	0	0	0	0	0	0
91.0	95	65	49	53	48	28	31	31	25	23	20	14	1	0	0	0	0	0	0	0
101.0	75	55	43	41	43	30	32	31	27	25	24	14	12	3	0	0	0	0	0	0
111.0	28	47	38	39	41	32	32	31	25	21	17	15	17	6	0	0	0	0	0	0
121.0	9	33	29	33	36	32	33	27	29	25	21	19	18	6	0	0	0	0	0	0
131.0	0	20	29	35	32	26	32	34	24	20	19	20	20	5	0	0	0	0	0	0
141.0	0	11	32	27	33	34	38	33	25	23	21	17	16	5	8	0	0	0	0	0
151.0	0	8	28	23	33	24	34	28	26	18	22	20	15	10	11	0	0	0	0	0

INITIAL EVENTS=100000 FINAL EVENTS= 20888

0.0	5.000	5.000	0.0	0.150	0.150	0.457	0.457				
1.000	0.325	0.0	0.0	151.000	-1.000	0.0	20.000				
0.09140	0.09140	0.09140	0.03000	0.03000	0.03000	0.01987	0.0	0.09620	0.15901	0.54901	0

magnet and the spectrometer is 3 meters away from the exit side. The case in Table IV (b) is with the target placed at the entrance of the analyzing magnet and the spectrometer set 5 meters away from the exit. The spectrometer module is displaced by about 0.5 meter from the straight ahead beam line. It is evident that by changing the target position inside the analyzing magnet and by setting the spectrometer modules at various locations several acceptance regions are defined selectively, for the purpose of observing particles in singles or in pairs.

Configuration II is designed to observe in pairs the production of wide angle leptons and gamma-rays. This is shown in Fig. 9. The beam and also forward produced charged or neutral particles are not observed by the spectrometer modules. Thus, a very favorable configuration is obtained which accepts the production of large angle and high energy charged particles or gamma-rays. The spectrometer modules are placed symmetrically, as it is seen in Fig. 9. The reactions to be studied by this configuration are also stated in this figure.

In Fig. 10, the spectrometer system for the studies of forward produced multi-gamma-ray final states is shown.

Thus, a versatile facility is provided at NAL by our modular spectrometer configurations. Both large angle and small angle emerging $e^{\pm}$, $\mu^{\pm}$, and γ particles can be observed in coincidences or in singles.

3. Detection of Showers Induced by Electrons and Gamma-Rays.

The spectrometer modules, in both our pion and electron experiments, are designed a) to observe several individual showers induced by electrons and gamma-rays, b) to provide a high rejection factor for hadrons and c) to observe and identify muons. Briefly, the detection system is based on the addition of multi-wire-proportional chambers (MWPC), having unique encoding

CONFIGURATION II

DESIGNED FOR WIDE ANGLE PRODUCTION OF LEPTONS AND PHOTONS IN PAIRS

$\pi^- N \rightarrow e^+ e^- +$ HADRONS

$\pi^- N \rightarrow \mu^+ \mu^- +$ HADRONS

$\pi^- N \rightarrow e^{\pm} \mu^{\mp} +$ HADRONS

$\pi^- N \rightarrow \gamma\gamma +$ HADRONS

NAL-PROTON LABORATORY
HIGH QUALITY ELECTRON / HADRON BEAM
40--300 GeV/c $\pi^-, K^-, \bar{p}$

OR

NAL-MESON LABORATORY
2.5 MRAD BEAM LINE
40--140 GeV/c $\pi^-, K^-, \bar{p}$

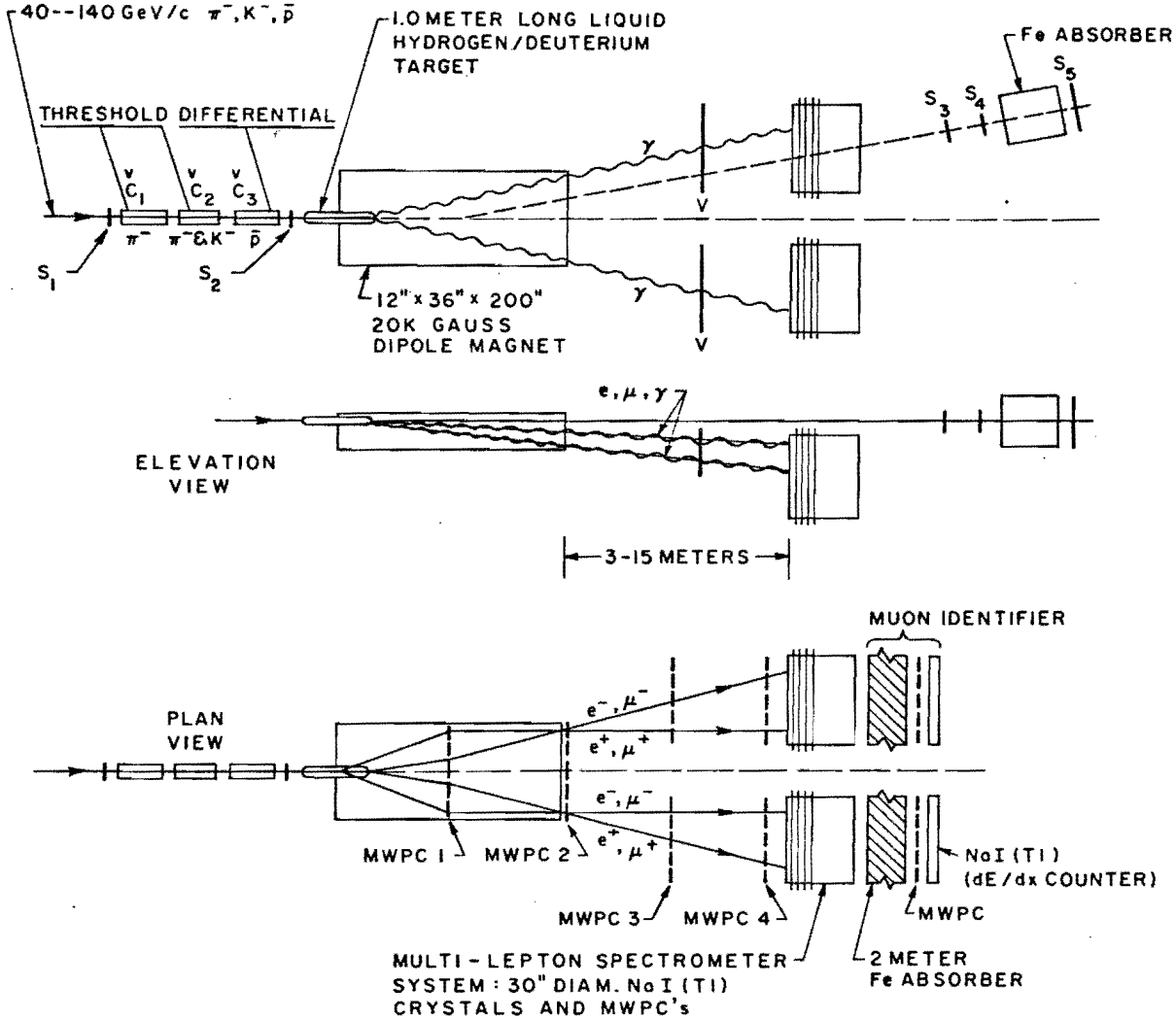

SCHEMATIC EXPERIMENTAL SETUP

(NOT TO SCALE)

Figure 9

CONFIGURATION III

FOR THE STUDIES OF MULTIGAMMA RAY FINAL STATES

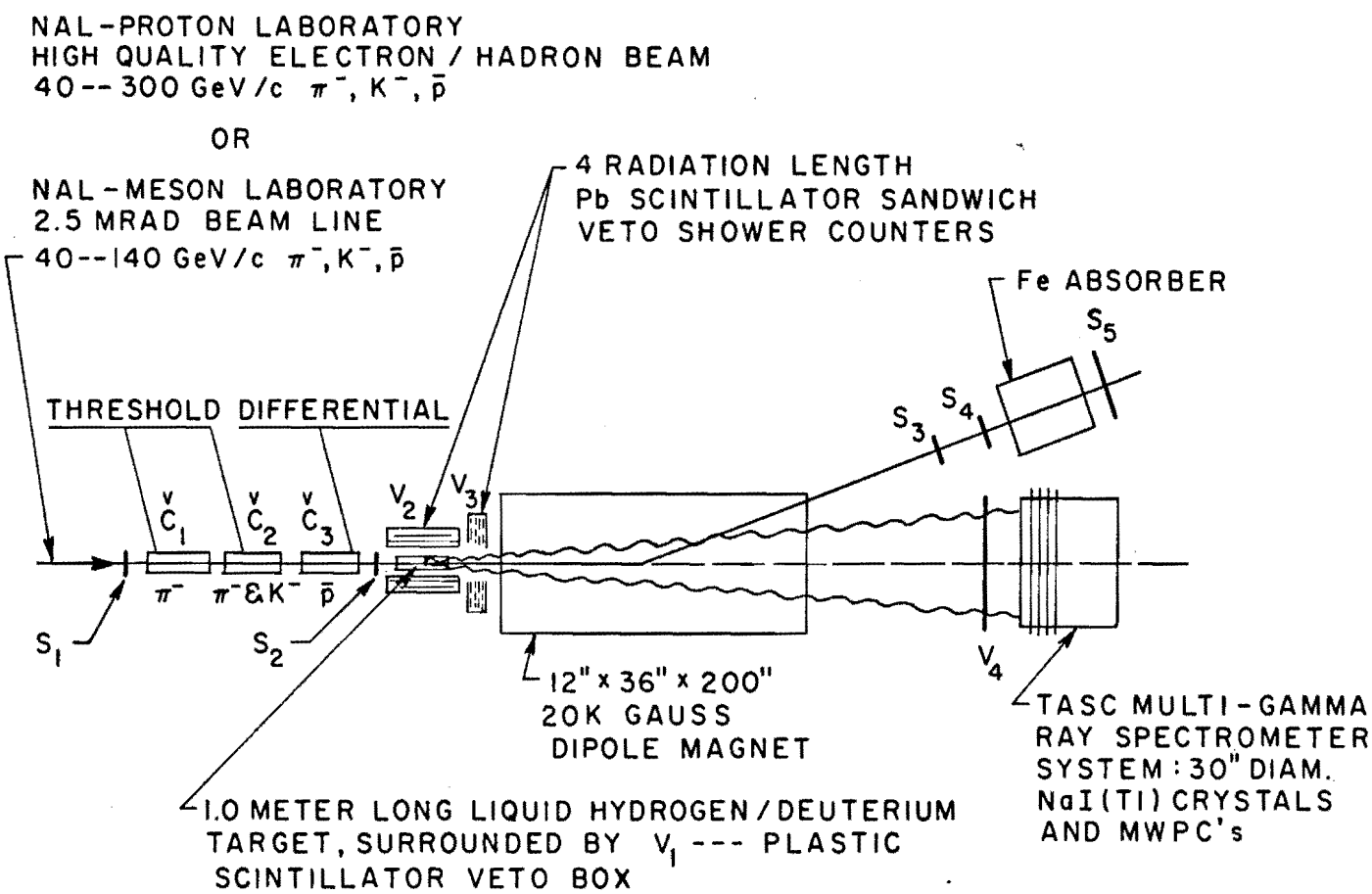

SCHEMATIC EXPERIMENTAL SETUP

(NOT TO SCALE)

Figure 10

and readout properties, to large NaI(Tl) crystals which are segmented in an especial arrangement.

We demonstrate the results of our recent tests and continuing development effort on MWPC's with electromagnetic delay line readout. Multi-tapped delay lines are used with fixed (5-10 nsec delay per tap) time delays between each chamber wire pairs. An intercepted shower induces signals over several wires. The overall sum signal of a shower propagates to the end of the delay line with a chosen and fixed speed (20-40 nsec/cm). These signals describe the shape of intercepted showers. They contain information on the space location of showers and shower electron multiplicities. In Fig. 11 the shape of 10 GeV electron induced showers is shown at several shower depth positions. In Fig. 11 (a,b,c) the individual signals are induced by electron showers generated by 1 X_o (radiation length) of lead. The statistical fluctuations in shower multiplicities are evident in these representative samples. At 10 GeV, the showers reach the maximum electron multiplicities in lead at about 5 X_o. These are depicted in Fig. 11 (d,e,f). A shower signal with 6 X_oPb is shown in Fig. 11 (g) and those with 4 X_oPb are in Fig. 11 (h,i). Several thousands of individual showers were observed in recent tests at SLAC. These signals are encoded with an electronics system which measures both the position of the center-of-charge and the amount of total charge. Both analog and digital information are made available by the electronics. The regions of individual shower signals are defined by time-over-threshold discriminator gates. These are also shown above in Fig. 11.

These results make it convincing that our continuing development effort will be successful in producing a working system for the observation of multi-gamma-ray and multi-lepton final states at NAL. The pair resolution

10 GeV ELECTRON SHOWERS ENCODED BY MWPC DELAY LINE AT 40 n sec/cm

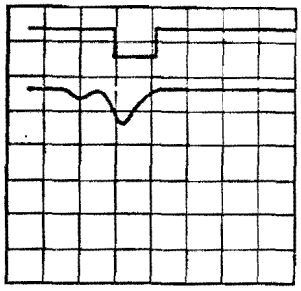

(a) $1X_0$(Pb), y = 0.5 V/cm

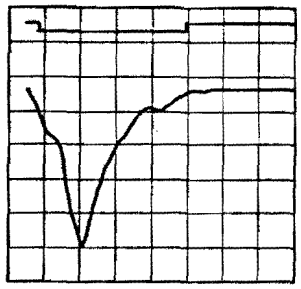

(d) $5X_0$(Pb), y = 5 V/cm

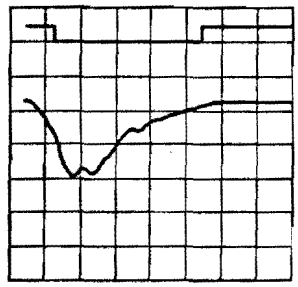

(g) $6X_0$(Pb), y = 1 V/cm

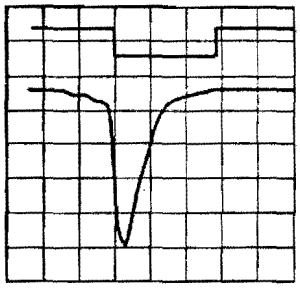

(b) $1X_0$(Pb), y = 0.5 V/cm

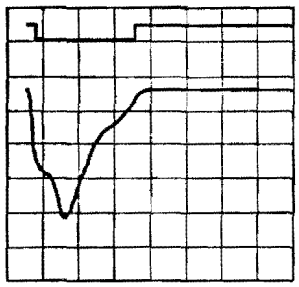

(e) $5X_0$(Pb), y = 3 V/cm

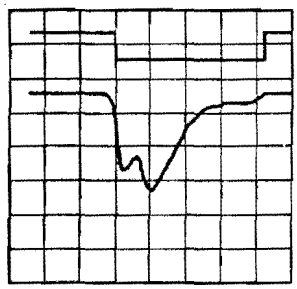

(h) $4X_0$(Pb), y = 1 V/cm

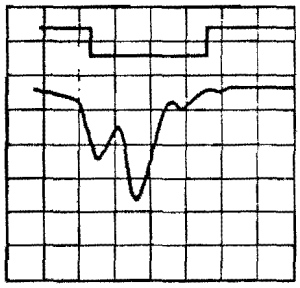

(c) $1X_0$(Pb), y = 0.5 V/cm

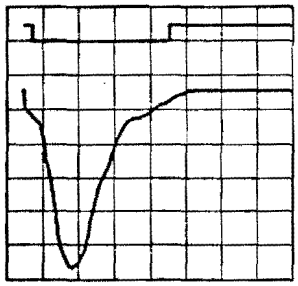

(f) $5X_0$(Pb), y = 2 V/cm

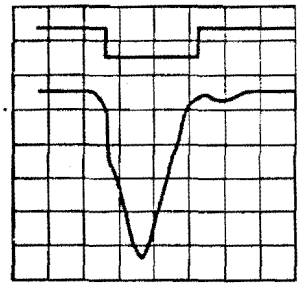

(i) $4X_0$(Pb), y = 1 V/cm

(x-AXIS SCALE IS 200 n sec/cm)

Figure 11

of induced signals, up to 10-12X_0 shower depths, is limited only by the natural widths of showers. At NAL energies these widths are narrowing (2-3 cm) and the electron multiplicities in showers are increasing (several hundreds of electrons at shower maxima). Therefore, the task of observing multi-gamma-ray and multi-lepton final states in a single large detector becomes easier at NAL than in the above tests carried out at SLAC.

4. Muon Identifiers

Muon identifiers will be included in our spectrometer modules. These are necessary in both of our electron and pion experiments. A simple muon identification method will be used, based on the total absorption of hadrons and electromagnetic showers: 30 radiation length of NaI(Tl) crystals and about 10 pion collision length of iron. The attenuation length of pions in iron is measured[21] to be 21 cm, so that a 2 meter iron absorber is sufficient to attenuate hadrons down (together with about 4 collision length in NaI(Tl)) to a level of below 10^{-6}. Muons are transmitted through the overall spectrometer module thickness and suffer ionization energy loss. Their trajectories are displaced by Coulomb multiple scattering. The energy loss is 2.7 GeV and the rms displacement of trajectories is about 0.4 cm for 50 GeV muons. The source of muon production is well defined by the small target volume and the small spot size of the incident beam.

Multi-wire proportional chambers are placed before and after the iron absorber. A 2 inch thick scintillator element is the last detector in the spectrometer modules. This is used to observe the overall ionization energy loss signal of transmitted particles. Thus, muons are identified and their trajectory is measured by the muon identifier elements shown in the figures of the experiment configurations.

5. Errors.

Well known formalisms and precise computations are used to arrive at the measurement uncertainties in our spectrometer configurations. The total errors are estimated for the determination of momentum p and production angle θ of produced charged particles. These errors are due to space coordinate measuring accuracy and Coulomb multiple scattering. In space coordinate measurements, conservatively a 0.5 mm uncertainty is assumed for each of the MWPC planes. The dominant effect due to beam spot sizes is also investigated. These are very relevant to our experiments for the spectrometer configurations we have discussed.

We demonstrate the improvement obtained with small beam spot size, in the accuracy of p and θ measurements. In Fig. 12 the total uncertainty in momentum measurement is shown, as a function of p, using the $\pm$2 mm spot size of our proposed beam. Also shown is the result with a $\pm$12 mm beam spot size which is representative of another beam. The measurement method is pictorially demonstrated in the insert of this figure. Similarly, in Fig. 13, the total uncertainty in scattering angle measurements is shown, as a function of p. Both p and θ measurements and errors are correlated. In this figure, the improvement derived from a small beam spot size definition is evident.

We argue that improvements in errors are made possible because additional information is available in our experimental spectrometer configurations. The new information comes from the precise energy determination in the case of electrons (and also gamma-rays). The information is obtained from the observed pulse heights from signals induced in the NaI(Tl) crystals of our spectrometer modules. During the analysis phase of our experiments, produced charged particles are grouped in

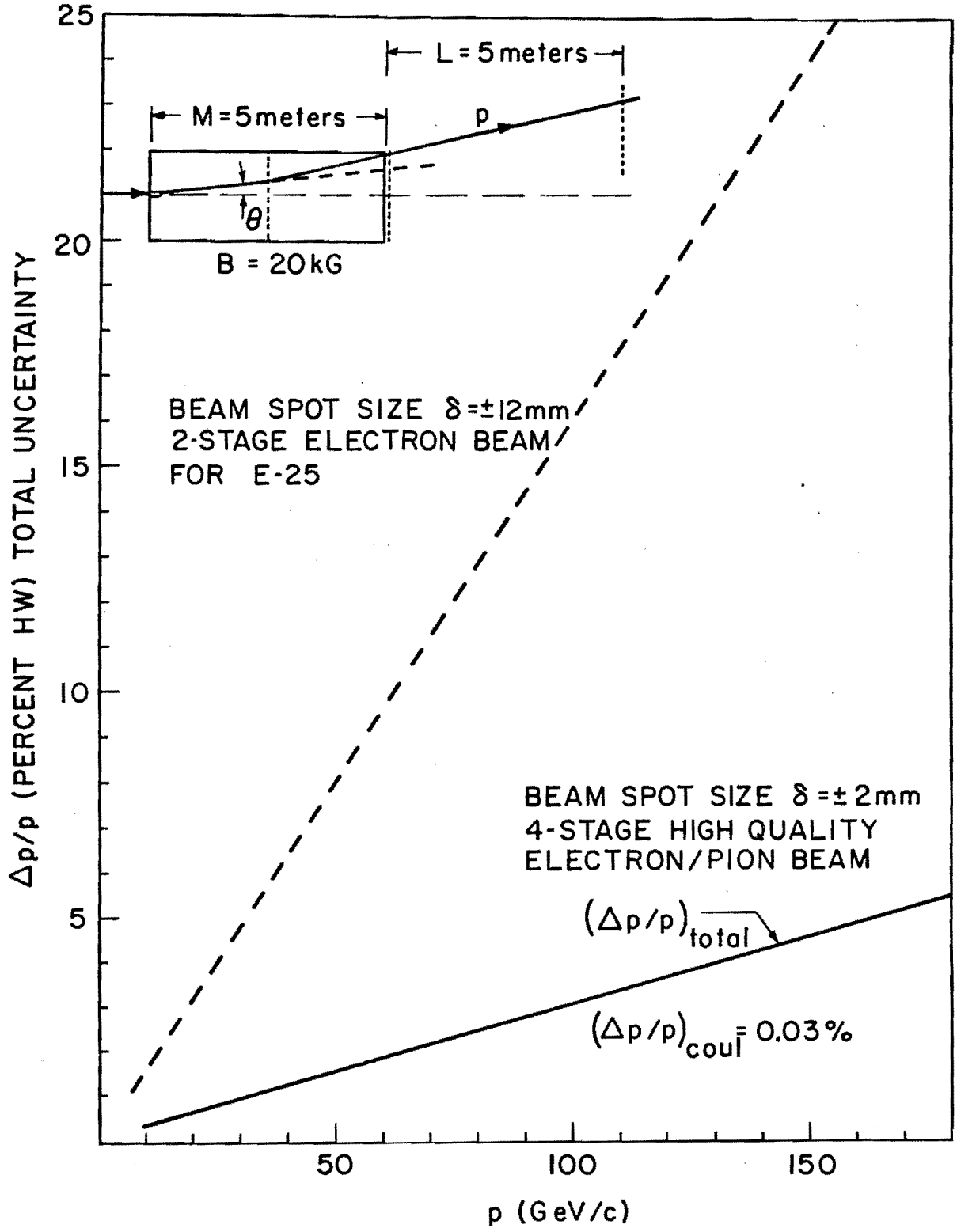
25
20
15
10
5
Δp/p (PERCENT HW) TOTAL UNCERTAINTY
L = 5 meters
M = 5 meters
p
θ
B = 20 kG
BEAM SPOT SIZE δ = ± 12mm
2-STAGE ELECTRON BEAM
FOR E-25
BEAM SPOT SIZE δ = ± 2mm
4-STAGE HIGH QUALITY
ELECTRON/PION BEAM
(Δp/p)total
(Δp/p)coul = 0.03%
50
100
150
p (GeV/c)

Figure 12

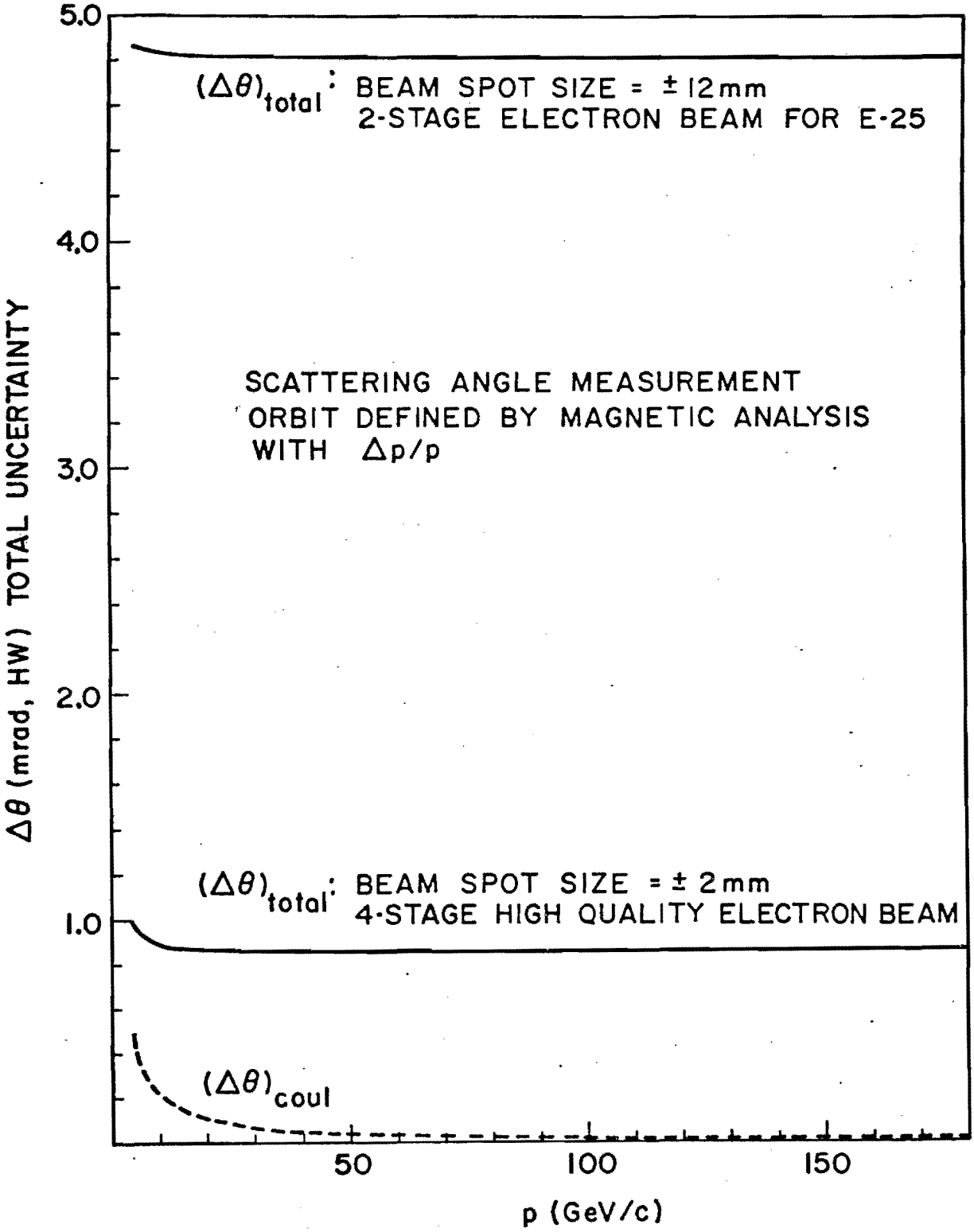
5.0
4.0
3.0
2.0
1.0
Δθ (mrad, HW) TOTAL UNCERTAINTY
(Δθ)total: BEAM SPOT SIZE = ± 12mm
2-STAGE ELECTRON BEAM FOR E-25
SCATTERING ANGLE MEASUREMENT
ORBIT DEFINED BY MAGNETIC ANALYSIS
WITH Δp/p
(Δθ)total: BEAM SPOT SIZE = ± 2mm
4-STAGE HIGH QUALITY ELECTRON BEAM
(Δθ)coul
50
100
150
p (GeV/c)

Figure 13

selected momentum bins. Momentum bin sizes are set by the above uncertainties for $\Delta p/p$. For each momentum bin, the spectrum of pulse heights from the NaI(Tl) crystals is examined. As we already know, each spectrum will show a clear and separated electron peak. Thus, electrons are identified. Moreover, a precise energy measurement is now available from the observed pulse height values. Using this precise energy measurement of identified electrons we will improve the errors in θ by means of the well known (E,θ) correlations. This improvement is demonstrated in Fig. 14. Therefore, in the case of observed electrons in our spectrometer modules, the final error in θ, will be $\Delta\theta \simeq$ 0.1 mrad. The same error values also apply for gamma-rays. In this case there are no (p,θ) correlations and the θ_γ errors are determined only by space coordinate uncertainties.

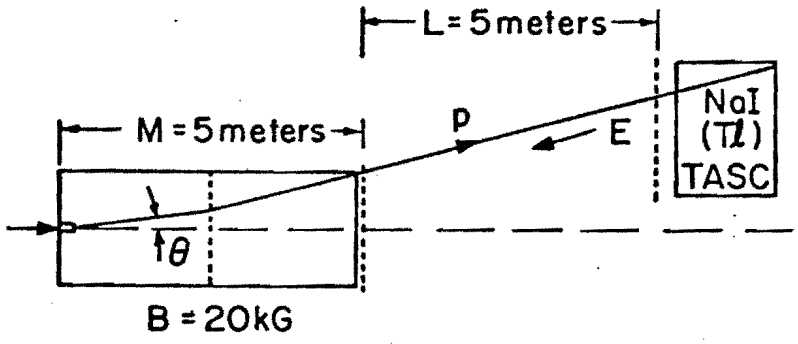

SCATTERING ANGLE MEASUREMENT

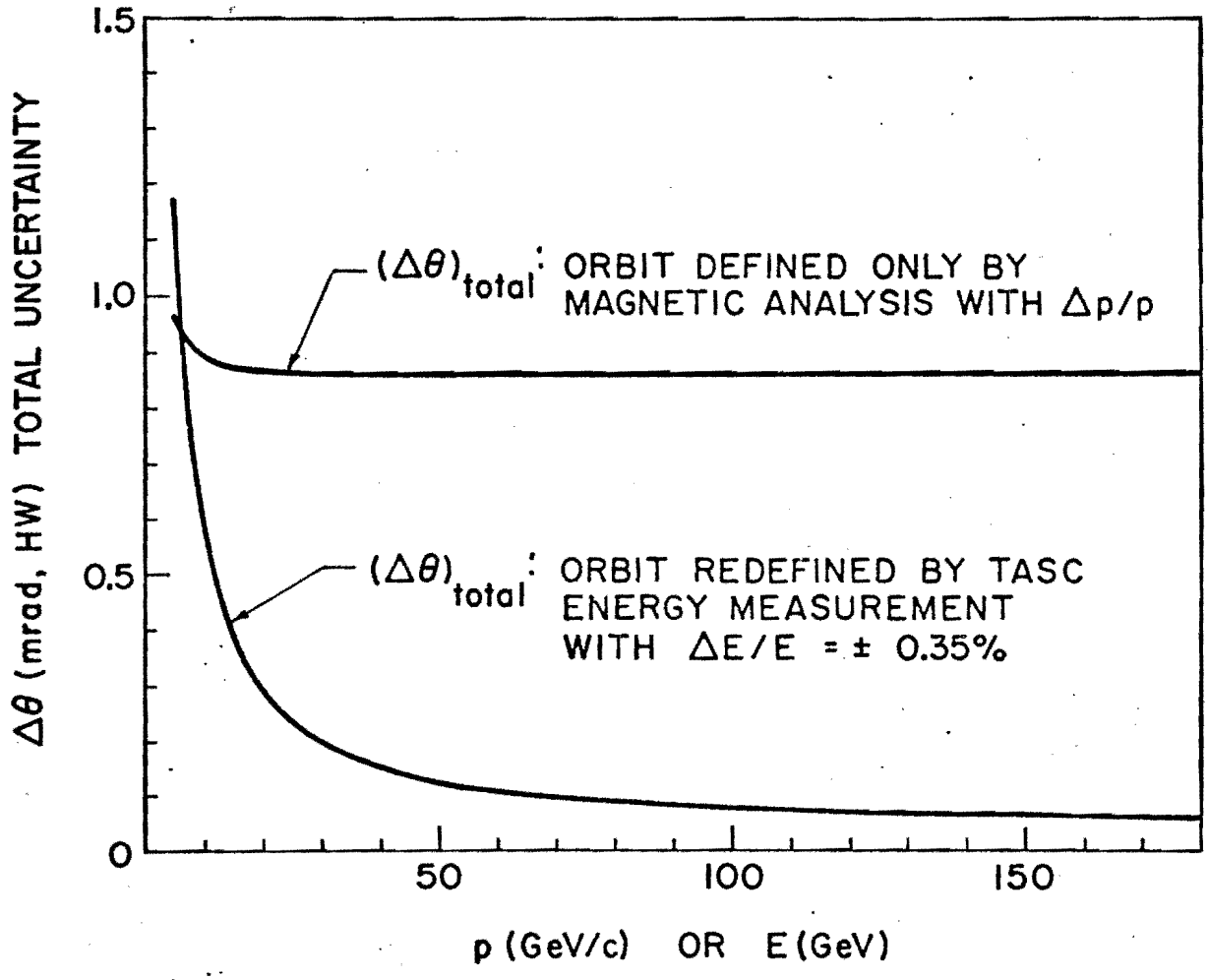

Figure 14

SUMMARY OF PROPOSAL REQUIREMENTS

1) This experiment requires no more than an external proton beam of 10^{12} protons/pulse incident on a secondary beam Be target.

2) 1100 hours of running time are required to complete the physics for this proposal. An additional 150 hours of equivalent beam time is estimated, for the purposes of experiment setup and equipment checkout during a period of 2 months.

3) To accomplish the proposed goals, the group of experimenters making this proposal will be augmented by three postdoctoral physicists and several graduate students. Other interested physicists are invited to join the group as collaborators.

4) The experimental equipment designated in this proposal requires a development and preparation time of a minimum of 20-22 months. Due to the commonality of experimental equipment in both the proposed electron and pion experiments, this preparation time will suffice for both proposals.

5) Other desired requirements to implement this experiment are discussed in the proposal. These are connected with beams at NAL and the cryogenic system for our targets and a superconducting magnet.

REFERENCES

1. S. M. Berman, J. D. Bjorken and J. B. Kogut, Phys. Rev. D4, 3388 (1971).

2. The CERN - COLUMBIA - ROCKEFELLER Collaboration data, presented by R. Cool at the XVI International Conference on High Energy Physics, Chicago-NAL, September 1972.

3. R. P. Feynman, Phys. Rev. Lett. 23, 1415 (1969) and in "High Energy Collisions", ed. C. N. Yang, Gordon and Breach, 1969, p. 237.

4. a) R. Blankenbecler, S. J. Brodsky and J. F. Gunion, SLAC-PUB-1140 (October 1972) to be published in Phys. Letters.

   b) J. F. Gunion, S. J. Brodsky and R. Blankenbecler, Phys. Letters 39B, 649 (1972); and SLAC-PUB-1053 (to be published in Phys. Rev.);

   c) R. Blankenbecler, Lecture Notes, McGill University Seminar, August 1972.

5. J. H. Christenson, G. S. Hicks, L. M. Lederman, P. J. Limon, B. G. Pope and E. Zavattini, Phys. Rev. Lett. 25, 1523 (1970).

6. S. Drell and T. M. Yan Phys. Rev. Lett. 25, 316 (1970); Ann. Phys. (N.Y.) 66, 555 (1971).

7. Yung-Su Tsai, Phys. Rev. D4, 2821 (1971).

8. J. D. Bjorken and C. H. Llewellyn Smith, SLAC-PUB-1107 (September 1972) to be published in Phys. Rev.

9. a) T. D. Lee and G. C. Wick, Phys. Rev. D2, 1033 (1970); D3, 1046 (1971);

   b) T. D. Lee, Phys. Rev. Lett.25, 1144 (1970);

   c) T. D. Lee, Phys. Rev. Lett. 26, 801, (1971) and PHYSICS TODAY, 25/4, 23 (1972).

10. J. D. Bjorken, private communication, see also, C. M. Llewellyn Smith, SLAC-PUB-1039 (April 1972) unpublished.

11. S. M. Berman, BNL 16978 (CRISP-72-32) (June 1972) unpublished.

12. L. M. Lederman, a) BNL report and CRISP-71-29 (1971);
b) BNL 17092 (CRISP-72-43) (1972) unpublished.

13. L. M. Lederman and B. G. Pope, 27, 765 (1971).

14. a) BNL 16716, "200 GeV Intersecting Storage Accelerators", ISABELLE, (a Preliminary Design Study, May 1972);
b) SLAC-146 and LBL-750, "Particle Physics With Positron-Electron Proton Colliding Beams", PEP (April 1972);
c) R. R. Wilson, Report at the XVI International Conference on High Energy Physics, Chicago-NAL, September 1972.

15. W. D. Apel, J. Ausländer, M. Müller, G. Sigurdsson, H. M. Staudenmaier, E. Bertolucci, I. Mannelli, G. Pierazzini, P. Rehák, A. Scribano, F. Sergiampietri and M. L. Vincelli, Phys Letters, 40B, 680 (1972); and Phys. Letters 41B, 234 (1972).

16. M. Holder, E. Radermacher, A. Stande, P. Darriulat, J. Deutsch, M. Hansroul, S. Orito, J. Pilcher, C. Rubbia, P. Strolin, K. Tittel, A. Fainberg, G. Grosso-Pilcher and M. Scire, Phys. Letters, 40B, 141 (1972).

17. G. Neuhofer, F. Niebergall, J. Penzias, M. Regler, K. R. Schubert, P. E. Schumacher, W. Schmidt-Parzefall, K. Winter, Phys. Letters 37B, 438 (1971); and Phys. Letters 38B, 51 (1972).

18. a) R. N. Cahn, SLAC-PUB-1087 (August 1972) to be published in Phys. Rev. Lett.
b) S. R. Choudhury and P. Rotelli, IC/72/113, Trieste (September 1972).

19. Z. G. T. Guiragossián and R. E. Rand, HEPL-677 and NAL-75 (October 1972) to be published in Nucl. Inst. and Meth.

20. L. Caneschi and A. Pignotti, Phys. Rev. Lett. 22, 1219 (1969).

21. F. A. Harris, S. I. Parker, V. Z. Peterson, D. E. Yount and M. L. Stevenson, Nucl. Instr. Meth. 103, 345 (1972).